ARCTIC ACOUSTIC MEASUREMENTS AT 50 kHz

APL-UW 7313

31 August 1973

APPLIED • PHYSICS • LABORATORY

A DIVISION OF THE UNIVERSITY OF WASHINGTON

CONTRACT N00017-71-C-1305

ARCTIC ACOUSTIC MEASUREMENTS AT 50 kHz

by R. E. Francois
W. E. Nodland

APL-UW 7313

31 August 1973

CONTRACT N00017-71-C-1305

CONTENTS

	Page
INTRODUCTION	1
EXPERIMENTAL METHODS AND FIELD PROGRAM	2
Experimental Methods	2
Experimental Field Program	7
DATA ANALYSIS AND RESULTS	13
General	13
Properties of the Reflected Signals	18
Results	18
Discussion	19
Attenuation Coefficient	31
Measurement	31
Results	32
Discussion	32
SUMMARY	34
REFERENCES	35

ACKNOWLEDGMENTS

The experimental program described in this report was complementary to the UARS development program sponsored by the Defense Advanced Research Projects Agency and monitored by the Office of Naval Research. It was initiated in early 1972, only a few months prior to the arctic operation, and fiscal support was provided by the U.S. Naval Ordnance Laboratory, with direction from Mr. M.M. Kleinerman, Arctic Project Manager for that Laboratory. The successful performance of the UARS system was essential to carrying out the experimental program and the authors wish to express our appreciation for the early expression of confidence evidenced by the Navy sponsor in providing the modest, but necessary funding which enabled this experiment to be prepared and the results to be analyzed and presented.

ABSTRACT

An acoustic transmission experiment was conducted in conjunction with development operations of the Unmanned Arctic Research Submersible (UARS) system off Fletcher's Ice Island (T-3). Transmissions from a low directivity, 50-kHz projector on the submersible (part of the UARS acoustic tracking system) were received at transducers suspended beneath the ice and then recorded. The profile of the ice immediately above the UARS was measured throughout the run and the UARS acoustic tracking system provided complete knowledge of the changing measurement geometry. The data were analyzed to yield the amplitude reflection coefficient as a function of the nominal grazing angle with the ice undersurface and the shift in reflection area, the sea water attenuation coefficient, and signal fluctuation statistics. The amplitude reflection coefficient was found to be highly variable and independent of grazing angle for angles from 10° to 40°; the reflected signal had short-term fluctuations with a standard deviation on the order of 5 dB. The mean coefficient, however, varied about unity by typically ±6 dB in a somewhat periodic manner which was related to a secondary 50 to 100 foot wavelength component present in the measured ice roughness spectra. The measured attenuation coefficient at a frequency of 50 kHz, a temperature of -1.62°C, a salinity of 31.9‰, and a pressure of 4.8 atmospheres was 11.0 dB per kiloyard. This value confirms Greene's arctic measurements but is some 5 dB less than that predicted by Schulkin and Marsh. The standard error of this measurement was 0.72 dB, which indicates that over the ranges used in the experiment (500-yd maximum) the direct path signal fluctuations ascribable to the medium were small.

INTRODUCTION

Arctic operations related to the system development of the Unmanned Arctic Research Submersible (Refs. 1 and 2) by the Applied Physics Laboratory, University of Washington, provided a unique opportunity to acquire basic and new acoustic information in a frequency region of potential interest to the Navy for ordnance applications, under-ice navigation sonars, and cooperative acoustic tracking operations in ice-covered seas. The primary objective of the experiment discussed in this report was to provide an insight into the reflection of acoustic pulses at small grazing angles (the angle between the reflecting surface and the incident ray) from the undersurface of growing multi-year ice. This reflection phenomenon is extremely important to near-horizontal acoustic propagation close to the water-ice interface because the typical arctic positive sound velocity gradient causes an upward refraction of the sound rays, with the result that a significant portion of the useful acoustic energy may be reflected from the surface. At less than critical grazing angles, elementary considerations indicate that the amplitude reflection coefficient should have value of unity (0 dB) if the surface roughness is much smaller than the wavelength. However, the magnitude of the reflection coefficient from typical arctic multi-year ice and its variation with change in reflection area (as would occur in transmissions between two under-ice transducers, or equivalent, moving relative to one another) are presently unknown since little direct investigation of ice reflectivity has been made.

The most extensive reported work to define an amplitude reflection coefficient from a water-ice interface has been done by Langleben and Pounder (Ref. 3). Their measurements were made as a function of incident angle at discrete frequencies between 20 to 450 kHz with angle of incidence at 15° intervals. Specular reflection from a horizontal under-ice surface was assumed and the reported amplitude reflection coefficient was calculated as the ratio of the measured amplitude of the reflected path signal to that of the direct path signal along water paths of equal distance using the same transducers. The same reflection area was used for all measurements at all frequencies; whether or not the same results would apply to a different or contiguous area was not established. The answer to this question was the one to which our experiment was chiefly addressed.

Our experiment was limited to only one frequency, namely 50 kHz. In addition to deriving statistics on the reflected and direct path signal fluctuations from the propagation data, we also sought to determine the attenuation coefficient of the water from the direct path measurements. This is an important measurement since at this frequency existing predictive equations--for example, Schulkin and Marsh (Ref. 4) and Greene (see Ref. 5)--differ by some 5 dB/kyd for arctic medium conditions.

The presence of pressure ridge keels in the reflection zone was expected to cause cutoffs in the reflected signal. However, the UARS profiler system was expected to provide information on pressure ridge keel parameters as well as a measurement of the roughness of the "flat" ice between the ridges, and it was hoped that this information would allow separation of observed acoustic fluctuation phenomena into categories related to the under-ice morphology.

To summarize, the objectives of the experiment discussed in this report were to determine the amplitude reflection coefficient from the undersurface of growing multi-year sea ice at grazing angles of potential interest for operational sonar, and other, applications at a frequency of 50 kHz and to determine the appropriate statistics describing the fluctuation of this coefficient as a function of shift in the reflection zone. The water medium attenuation coefficient and direct transmission signal fluctuation statistics were also to be determined.

EXPERIMENTAL METHODS AND FIELD PROGRAM

EXPERIMENTAL METHODS

The experiment was conducted using the UARS system as the principal tool and, consequently, a description of the system as it applies to this experiment is in order. Briefly, the UARS system consists of an acoustic telemetry-controlled, torpedo-like vehicle which can operate under the arctic ice carrying acoustic and other research instrumentation (Fig. 1). An acoustic tracking system determines the position of a tracking projector mounted on the UARS at 2-sec intervals. Within a typical 2-mile diameter operating area the standard error of the position measurement is less than one foot relative to an established reference baseline. The 50-kHz tracking projector aboard the UARS was the acoustic source used in this experiment. This transducer is mounted directly under a multi-beam, upward-looking acoustic lens used in measuring the profile of the ice (see Fig. 2). The geometry applying to the profile measurement is shown in Fig. 3.

The standard error in absolute elevation of the under-ice surface arising from errors in measurement of depth pressure, atmospheric pressure, roll, pitch, two-way acoustic pulse travel time to the reflecting surface, water column velocity, water column density, and quantization effects is 0.27 foot. The largest error contribution at the 150-foot UARS operating depth used for this experiment arises from quantitizing effects and is 0.07 foot. Since the vehicle is very stable in depth-keeping, roll, and pitch, this value is an appropriate figure to consider in determining profiler system resolution limits with respect to surface

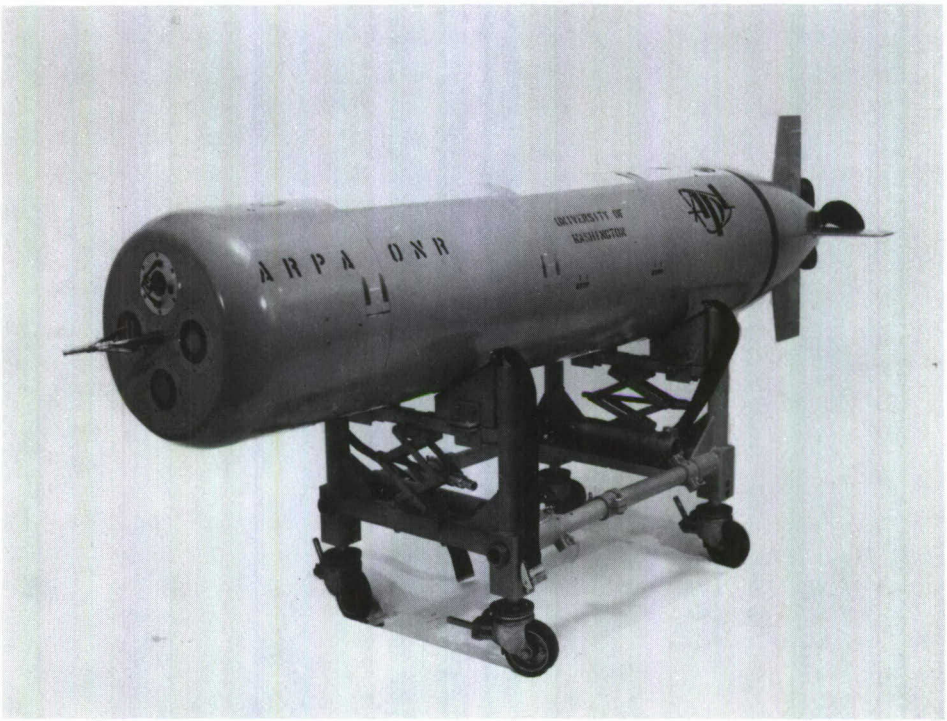

Figure 1. UARS on Vehicle Handling Dolly.

roughness spectra, viewed from an instrumentation standpoint. The under-ice reflecting surface itself, because of the loose-knit skeleton layer structure present during the freezing growth process, may be difficult to define. At 50 kHz the acoustic wavelength in sea water is approximately 1.2 in.--the same order of magnitude as the scatterers making up the skeleton layer. However, the experimental evidence is that, even though the exact depth of effective acoustic penetration into the skeleton layer is unknown, the uncertainity in that distance is small compared to the quantitizing error.

The geometry of the test area is illustrated in Fig. 4. Four tracking hydrophones (of no relevance to the experimental procedure aside from their position measuring function) were arranged in an approximate square about 3,000 feet on a side. (The tracking hydrophone buoys, frozen into the ice, relayed successive acoustic signals by radio link to the control hut.) Transducers mounted at ends of a reference baseline and connected by a coaxial cable to the control hydrohut were employed to measure the baseline length by acoustic means and to survey in the tracking hydrophone transducers. During the UARS run, the signal from the UARS tracking projector was received at each of the baseline transducers, which were cable connected to a preamplifier-calibrator and thence to a wide bandwidth, FM Sangamo tape recorder. Each transducer signal was recorded on two separate channels at different gain levels. Additional channels were used for time synchronization with the tracking system computer and

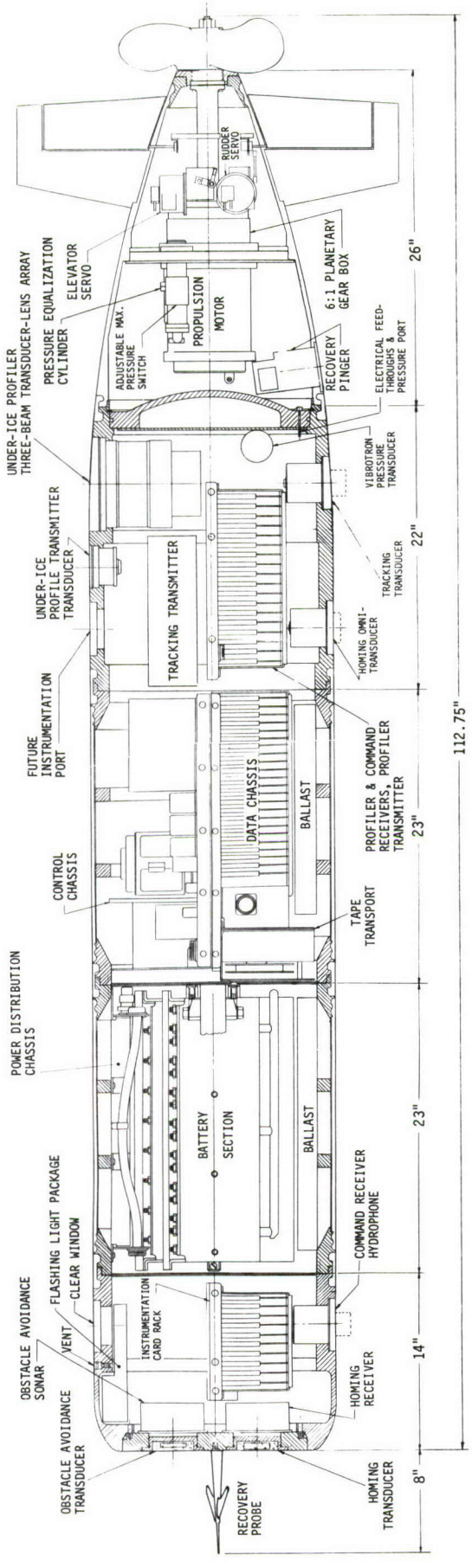

Figure 2. Cross-Sectional View of UARS

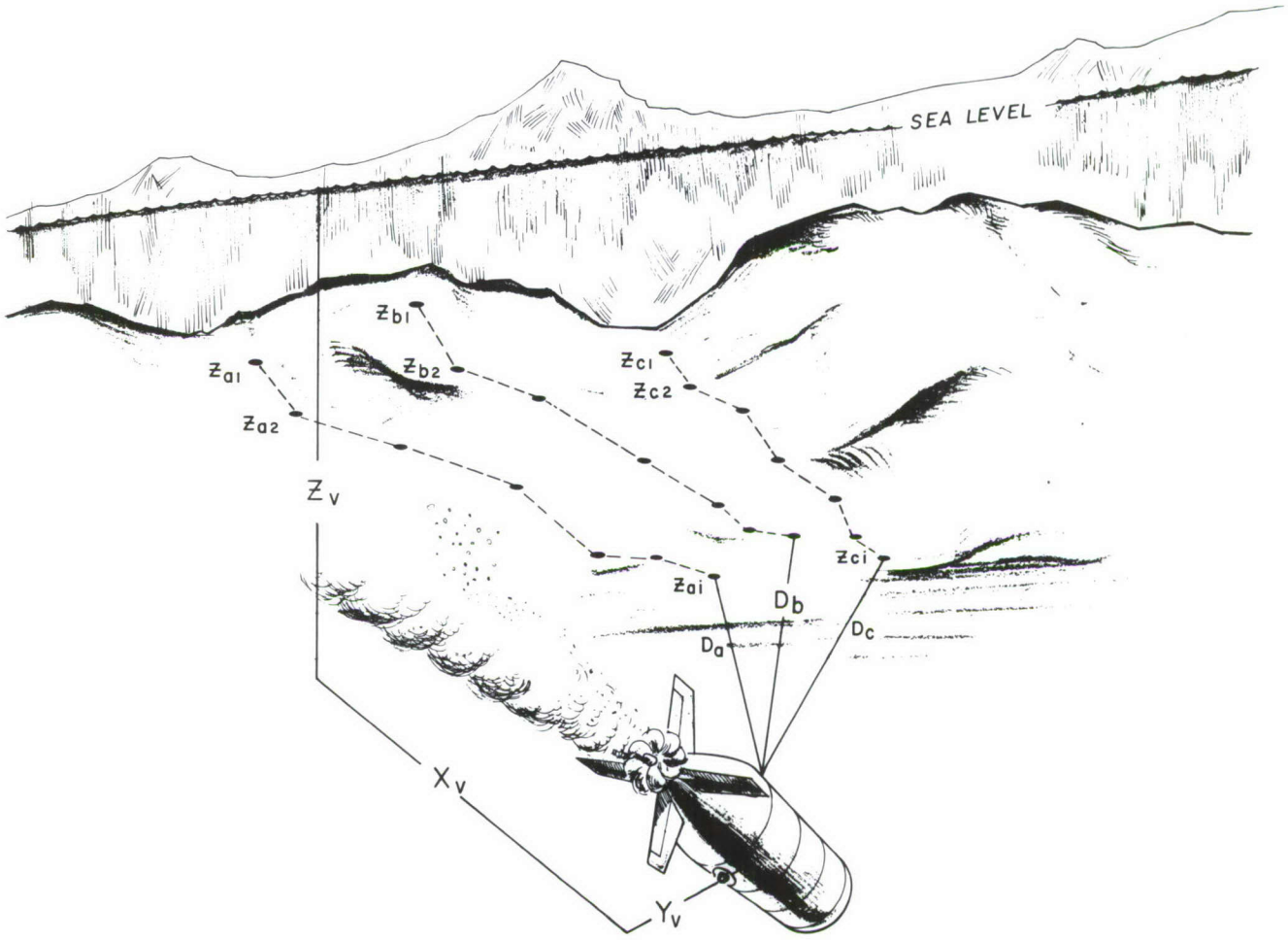

Figure 3. Measurement Geometry of UARS Profiling System.

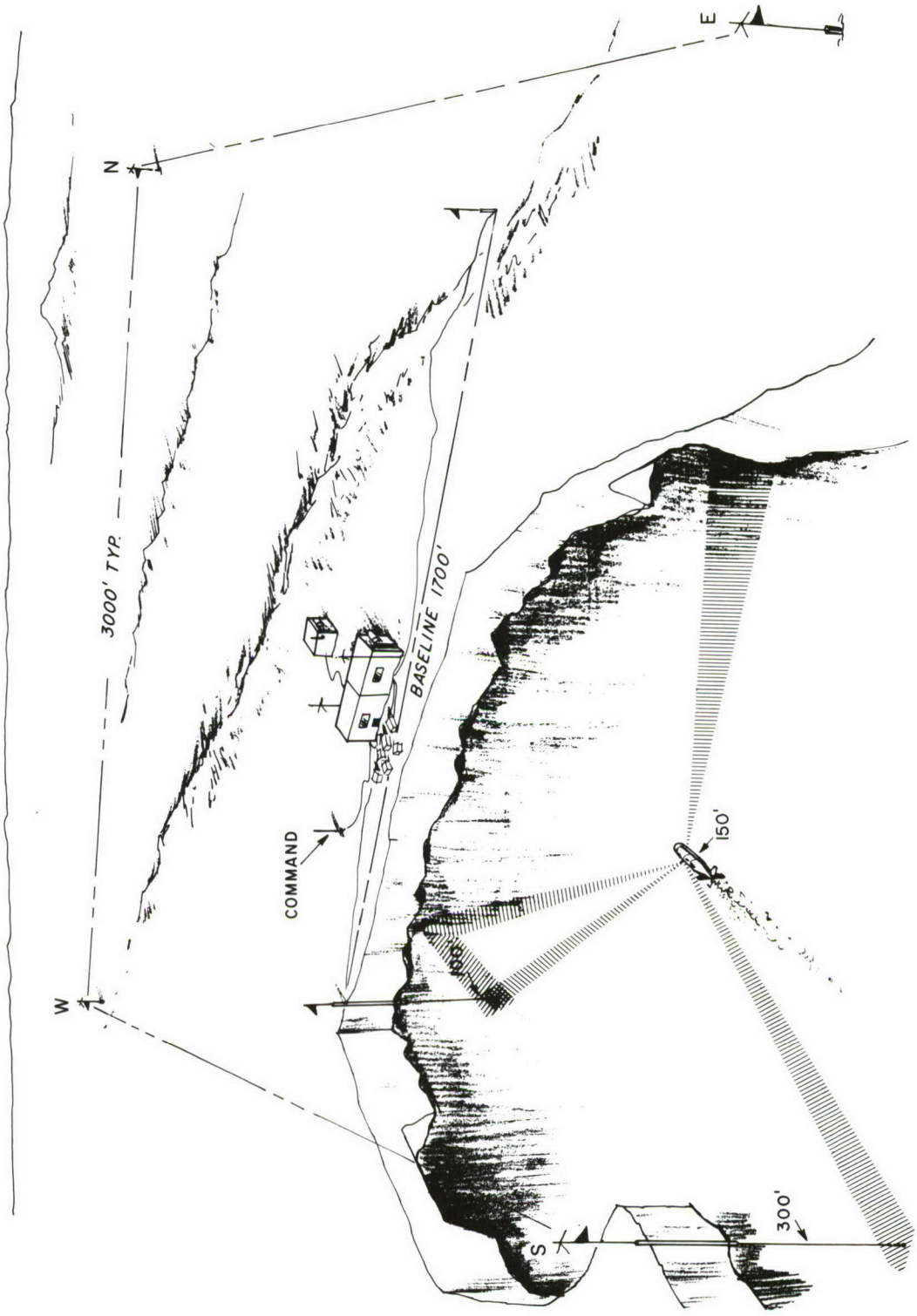

Figure 4. Test Area Geometry.

for voice annotation. The 50-kHz acoustic pulse from the tracking projector aboard UARS was phase-coded and the profile data were contained within the 1.3 msec pulse. As indicated in Fig. 4, the UARS projector depth (for this experiment) was 150 ft, the depth of the receiving transducers was 100 ft, and the nominal depth of the "flat" ice was 15 ft. Consequently, the direct and reflected path pulses arrived at the receiving transducer separated in time and without overlap out to ranges of about 1100 yd. According to the experiment plan, the UARS would be kept within 1000 yd of the baseline transducers throughout the experiment. This geometry would have restricted measurements to grazing angles between 4° and ~40°. However, in the actual experiment, signal-to-noise problems related to recorder-computer interaction restricted the range to a 500-yd maximum and hence the smallest grazing angle to ~7°. The direct and reflected acoustic transmission paths are illustrated in Fig. 4.

The data obtained at azimuth angles within ±80° of the UARS longitudinal axis, measured from the forward end, were not used in the analyses because of nulls in the projector directivity pattern at the elevation angles of interest. This perturbation was expected on the basis of previous experience with hull-mounted projectors of this type and, consequently, the run patterns were chosen to avoid on-axis azimuth angles to the baseline transducers. While the pressure of time in the UARS development program prevented obtaining actual three-dimensional beam patterns prior to the arctic experiment, these patterns were obtained after the field experiment and were employed in correcting the data for the directivity of the projector when mounted in the fully-assembled UARS vehicle.

EXPERIMENTAL FIELD PROGRAM

The UARS field development program was conducted at Fletcher's Ice Island (T-3) during April and early May of 1972. At that time, the island was essentially stationary near 84.5° North Latitude and 84.5° West Longitude. The temperature gradually increased from the -40°F typical of early April to near 0°F on 9 May, the day on which the data for this experiment were taken. The size and location of the operations area and the UARS trajectory relative to T-3 are shown in Figs. 5 and 6. As shown in Fig. 5, an old shear ridge lay along a line more or less tangent to the island. Inside of this pressure ridge lay Colby Bay. The ice in the bay was fast to the island and had been fast for approximately the preceding 8 years. The mean ice draft in the bay, from UARS measurements, was about 19 feet. The baseline transducers, labeled T_1 and T_2 in the figures, were the transducers used to receive the acoustic transmissions in this experiment. Within Colby Bay, the upper ice surface was unridged but was slightly lumpy due to ablation and melt-water erosion during the summer season. In early April the snow cover on the bay varied between a few inches and a few feet thick, masking almost entirely the ice surface. As the temperature warmed to ~0°F, ablation reduced

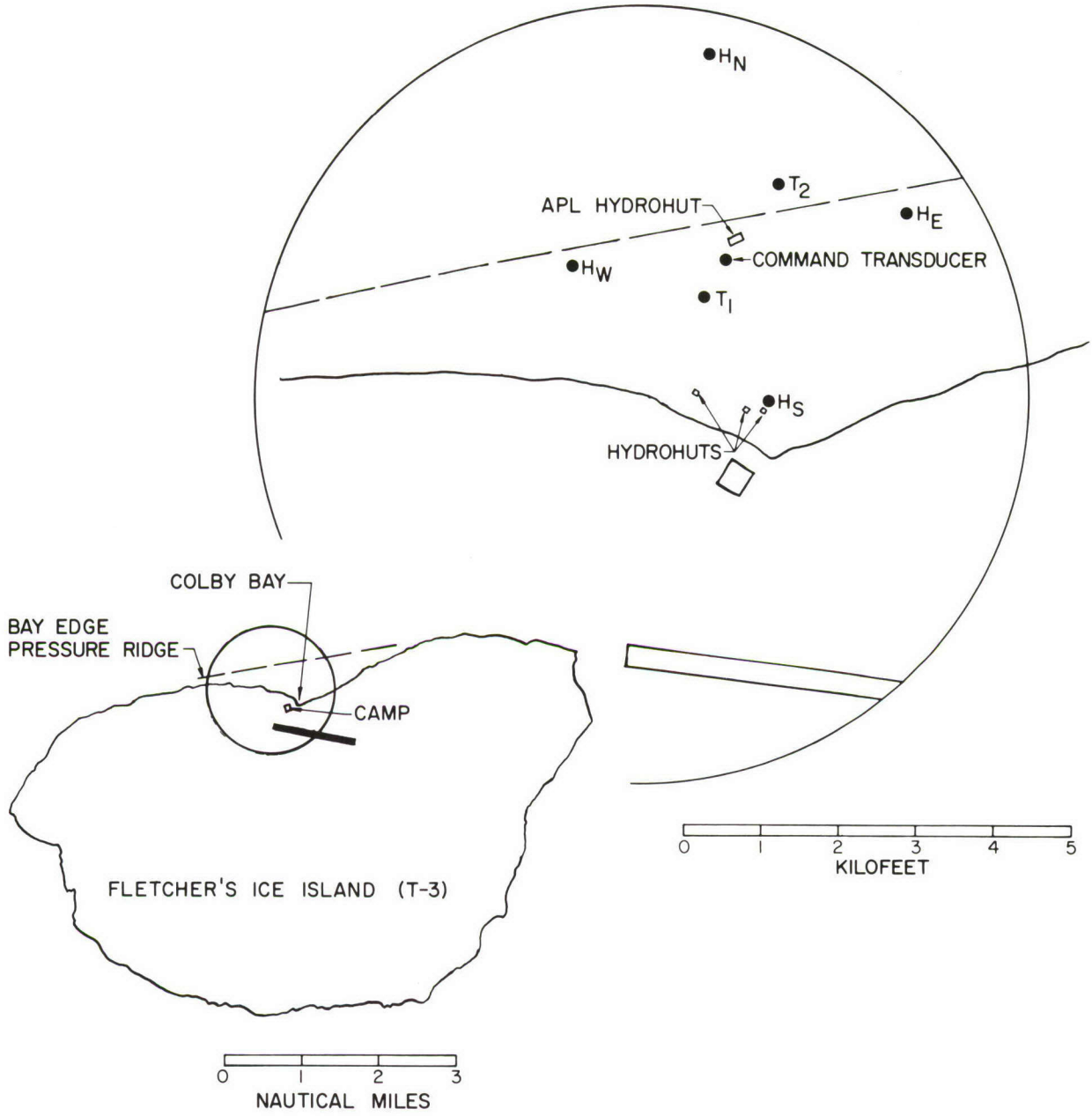

Figure 5. UARS System Geometry at Fletcher's Ice Island (T-3).

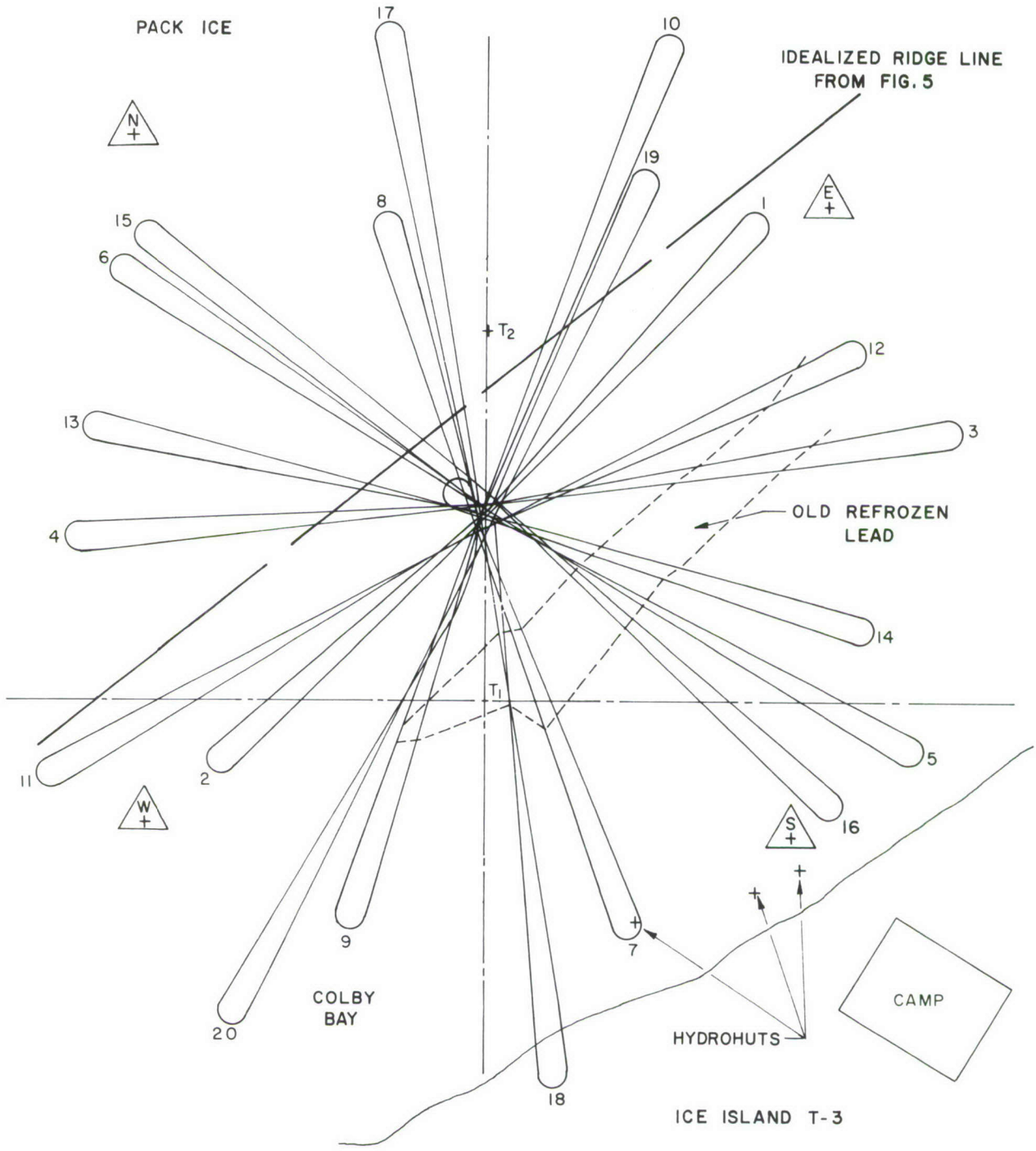

Figure 6. UARS Trajectory, 9 May 1972.

the snow cover significantly, but not enough to reveal the small-scale ice surface roughness that was apparent in late May. The outline of the old, refrozen lead with a draft of about 14.5 feet indicated in Fig. 6 is based on the profilometer data. At no time was the presence of this lead discernible from observation of the snow-covered surface. A level traverse made by conventional surveying techniques along a UARS track (lower line of the trajectory from run leg 5 to run leg 6 in Fig. 6) is shown in Fig. 7. Both ice and snow elevations were measured but only the ice elevations are plotted here. The plot has been broken up into three sections in order to better show the detail of both the upper and the lower ice surfaces. The lower surface of the ice is defined from discrete digitized measurements made 5 times per second by the profilometer. At a UARS speed of 3.7 kn, this rate corresponds to one measurement each 1.26 ft along the traverse. The refrozen lead is clearly identified in both the upper and the lower profile plots. The beam width of the vertical profilometer beam was slightly less than one degree; therefore, the diameter of the insonified area associated with each profilometer measurement was about 2 ft.

While the plot of Fig. 7 is based on the data obtained during the run in which the reflectivity experiment was conducted, our previous runs had provided similar information as to the nature of the under-ice topography both within Colby Bay and outside it in the pack ice. Thus the rough nature of the pressure ridge keels and vertical or re-entrant surfaces that can be noted in the profiles were known prior to this run. However, the possibility of obtaining useful reflections from these ridge keels, reflections that would contribute to further knowledge of the intrinsic variability of the reflected acoustic signals from the water-ice interface, was thought to be small since the bottoms of the ridge keels were very rough. Consequently, the run plan of Fig. 6 was designed to ensure data acquisition in sufficiently long sequences that flexibility in data analysis would not be compromised. This run plan dictated that somewhat more than half of the potential opportunities to collect water-ice interface data would occur in Colby Bay, which is representative of old (on the order of 10 years), multi-year ice. The remaining opportunities would be in the pack ice seaward of the bay, where ice of various ages was present. This variability can be observed in Fig. 7 from the progressively shallower ice drafts between pressure ridge systems as the distance from the island increases.

Prior to the experimental run, a conductivity-temperature-depth (CTD) measurement was made (see Fig. 8), as had been done for the previous 22 days. During this 23-day period, the island drift was slight, and currents in the region (Alpha Ridge) were small because of its location in a circulatory stagnation area. Consequently, little evidence of new leads was observed near the island and the stability of the water column properties in the depth region of interest to us was remarkable. A slight warming

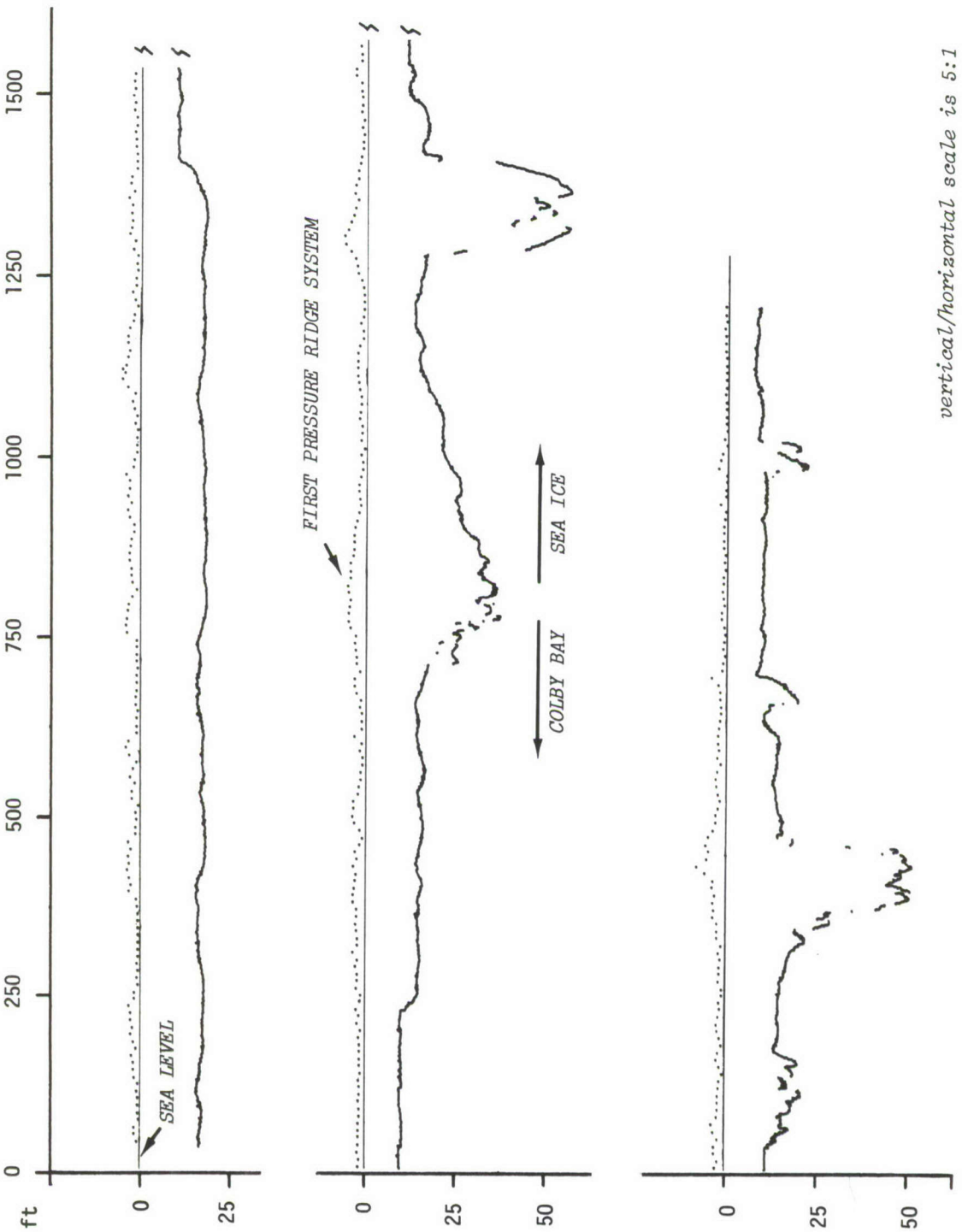

Figure 7. Upper and Lower Surface Profiles of Pressure Ridged Ice Measured During UARS Operation at Ice Island T-3 in Spring 1972.

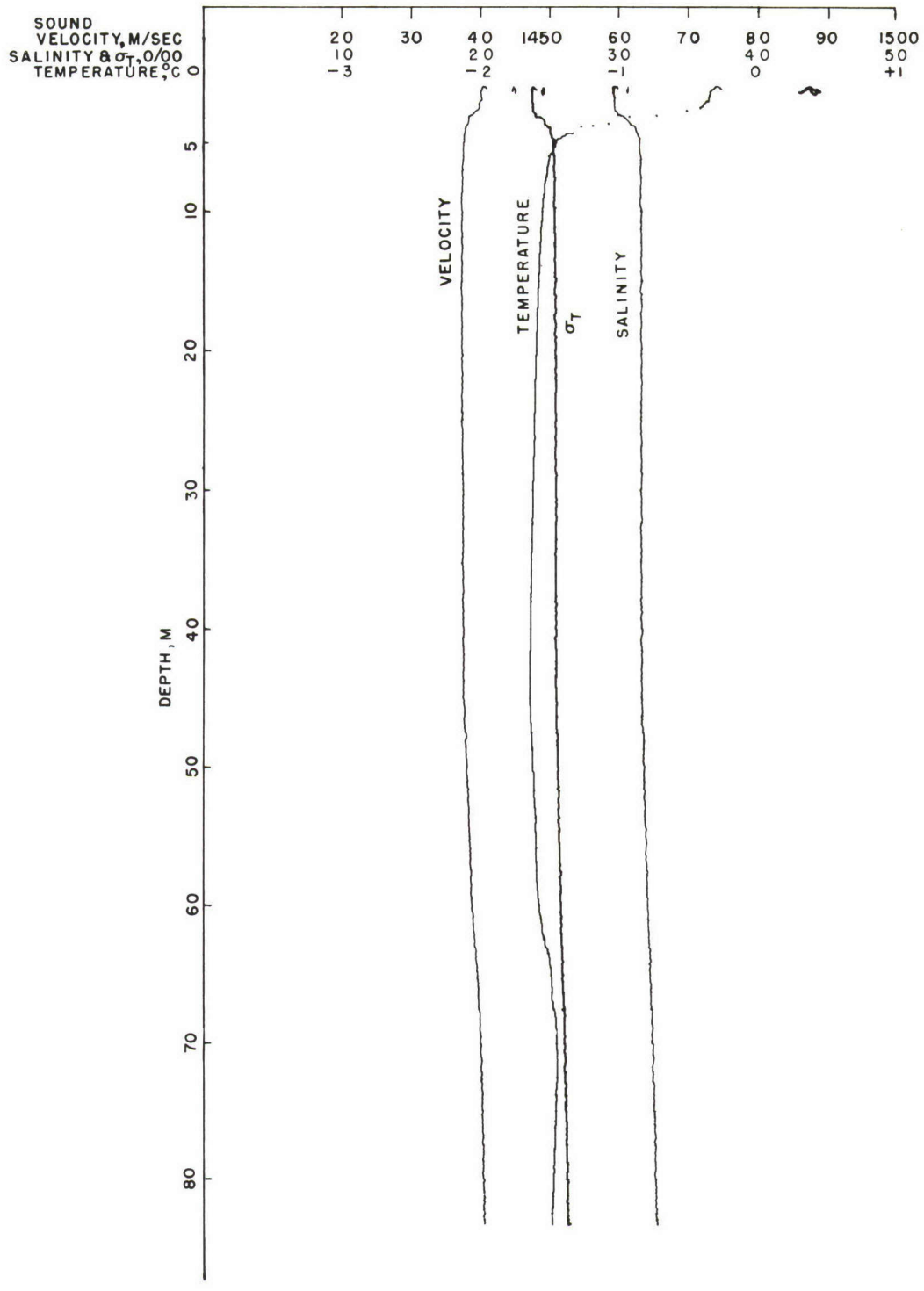

Figure 8. Vertical Profiles of Salinity, Temperature and Sound Velocity from CTD Measurements.

trend of perhaps 0.05°C was observed over the period that the CTD measurements were made. The only obvious differences in these measurements with time were confined to the hydrohole (4 ft x 12 ft x 28 ft deep), where we were supplying heat to prevent freezing. The plot shown in Fig. 8 is a copy of the digital plot prepared in the field from the direct digital recording of conductivity, temperature and depth. The density and sound velocity were computed from the measurements and these results were used in the tracking system computations, and the subsequent ice profile data reduction, acoustic refraction corrections, etc.

The reflectivity experiment run took place on 9 May 1972 and lasted 4 hours, during which time the UARS traveled 17.5 miles. The acoustic pulse data were recorded during the first two hours of the run, during which period the trajectory legs from 1 to 10 shown in Fig. 6 were completed. During the run, it was necessary to change the magnetic recording tape and also to use the measurement transducers, T_1 and T_2, for different purposes so that only 1-1/2 hours of data were actually obtained. A scan of the recorded data was made after the run and it was found that during the run crosstalk between a 50-kHz source (subsequently traced to the computer) and the signal lead had occurred. In some parts of the record, the noise level was high enough to interfere with the data, while in other sections the interference level was low. The result was that the useful dynamic range of the recording was limited to 25-30 dB and that some of the data were unusable because of the interference. The unusable data were correlated with the disconnection and reconnection of the transducers to the recording system but the lost data did not cause loss of extended sequential data sets. Three typical data sets were ultimately selected for detailed analysis.

DATA ANALYSIS AND RESULTS

GENERAL

The data upon which the analyses were based are enumerated below.

(1) computer time correlated FM recording of the acoustic signals received at the measurement transducers

(2) computer time correlated, digital internal recorder record of UARS giving roll, pitch, depth and distance to ice undersurface, at a data rate of five measurements per second

(3) computer time correlated, external record of UARS position with time at 2-sec intervals through the run

(4) sound velocity profile on day of experiment

(5) measured three-dimensional directivity patterns of the acoustic transducer in the assembled vehicle

(6) measured directivity patterns of the receiving transducers

(7) supplementary data required for system calibration purposes.

Following the field exercise, the complementary data relating primarily to operation of the basic UARS system were reduced. Three-dimensional directivity pattern measurements were made with the assembled UARS vehicle using the Laboratory's acoustic barge calibration facility. Sections of the acoustic recording were then selected for analysis, avoiding, whenever possible, regions with a significant slope in the directivity pattern at the elevation and azimuth angles corresponding to the measurement geometry. Two techniques were used for quantitizing the data. In the first technique, the data were re-recorded on a Concord TV tape recorder, then played through an appropriate repeater. This technique allowed stopping the recorder playback for detailed examination of the total pulse. The amplitude of the signal was read within the first 200 μsec of the leading edge of the 1.3 msec pulse. The time separation between the direct and reflected path pulses was also recorded. After some experience with this approach, a direct readout technique was employed, using a long persistent oscilloscope display and a straight run-through of the original tape recording. Direct and reflected pulses were read in individual sequences and the readings were voice recorded and time correlated. Each method had its advantage but the latter technique took less time and was therefore used to obtain the data sets upon which this report is based.

The amplitude reflection coefficient described in this report is identical in definition to that of Langleben and Pounder (Ref. 3), although the experimental method is quite different. When it is expressed in decibel form, this reflection coefficient can be thought of as the reflecting strength of the water-ice interface.

Consider the geometry in Fig. 9. The assumption is made that the reflection from the ice undersurface is specular. The signal level, SL, at the receiver is, for the reflected path transmission,

$$SL = S - \delta_t + R - \delta_r - H \qquad (1)$$

where

S = the on-axis source level of the projector

δ_t = the number of dB down (on the projector beam pattern) for off-axis transmission

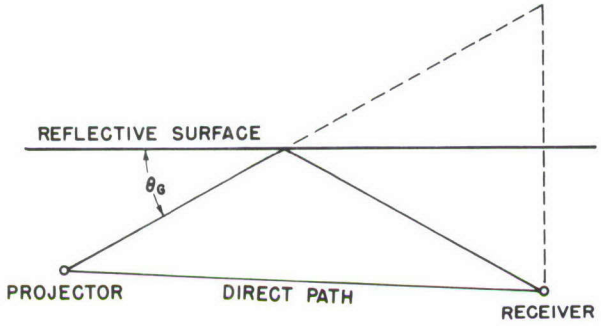

Figure 9. Geometry for Specular Reflection.

δ_r = the number of dB down (on receiving hydrophone beam pattern) for off-axis reception

R = the reflecting strength of the water-ice interface

H = the water path transmission loss.

Let the subscripts R and D denote the reflected and the direct path transmissions, respectively. The signal level at the hydrophone from the direct path transmission is then

$$SL_D = S - \delta_{tD} - \delta_{rD} - H_D \qquad (2)$$

and for the reflected path,

$$SL_R = S - \delta_{tR} + R - \delta_{rR} - H_R \quad . \qquad (3)$$

Taking the difference of the two equations, we have

$$SL_R - SL_D = - \delta_{tR} + \delta_{tD} - \delta_{rR} + \delta_{rD} - H_R + H_D + R \quad . \qquad (4)$$

SL_R-SL_D, expressed in decibels, is

$$20 \log \frac{V_R}{V_D} \quad ,$$

where V_R/V_D is the ratio of the amplitude of the reflected signal to that of the direct path signal, measured at the receiver hydrophone.

Substituting and rearranging terms, we have

$$R = 20 \log \frac{V_R}{V_D} + (\delta_{tR} - \delta_{tD}) + (\delta_{rR} - \delta_{rD}) + (H_R - H_D) \quad . \qquad (5)$$

Computed on an individual pulse basis, the value of R, then, is the measure of reflectivity sought. Its computation on a ping-by-ping basis allows the result to be independent of the absolute source level or the receiver gain setting during the experiment.

In order to make the corrections for transducer pattern directivity, the ray departure angles from the UARS projector were first computed as a function of the geometry. A variant of the SONAR ray tracing program (Ref. 6) was used to construct a refraction correction curve as a function of the range between the source and the receiver for both direct and reflected path rays--again assuming specular reflection at the water-ice interface. The spreading losses for both direct and reflected path rays were also computed, taking into account the small refraction effects. For the experimental conditions, the greatest departure from spherical divergence was computed to be less than 0.1 dB for ranges up to 1000 yd.

An attenuation coefficient of 13 dB per kiloyard was assumed during this part of the experiment analysis. (A somewhat smaller value based on experimental measurements of the direct path transmissions was later computed.) This assumption had negligible consequences since the attenuation loss over the small difference in the direct and reflected ray path distances was of little significance in evaluating R. The elevation angles determined from the ray trace computation and UARS roll and pitch combined with the UARS azimuth angle computed from position data were used for the double interpolation of the measured directivity pattern plots (azimuthal directivity plotted at fixed elevation angle increments). The receiving patterns of the hydrophones were omnidirectional in the azimuth plane and had only a slight vertical directivity variation, which was easily accounted for in the computational process.

Three sections of the UARS trajectory were utilized in determining the reflecting characteristics of the water-ice interface. These sections are plotted in Fig. 10, along with run leg 5-6, which was approximately perpendicular to the axis of the pressure ridge rows seaward of Colby Bay. The other, shorter, sections are numbered according to the general leg number given to each "spoke" of the run trajectory (see Fig. 6). In the analyses, the leg numbers are used to identify the data sets. In Fig. 10 the measurement transducers are labeled T_1 and T_2 and the arrows paralleling each leg indicate the direction of UARS motion. The dashed lines paralleling the UARS track and located toward the measurement transducer depict the line of advance of the reflection area. The data analyses in this report are derived from measurements made at transducer T_1 only.

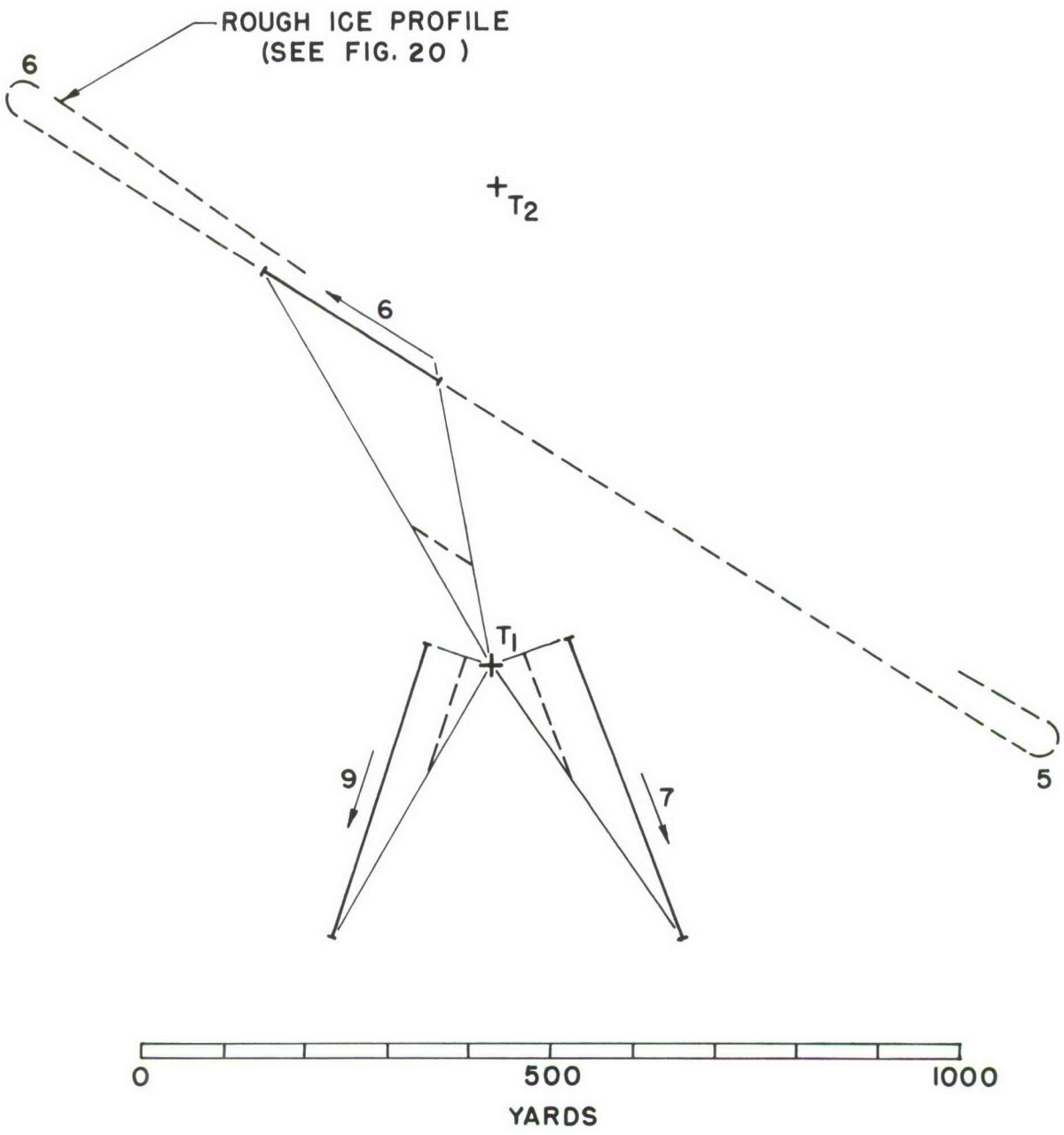

Figure 10. Trajectory Legs Corresponding to Acoustic Data Sets.

PROPERTIES OF THE REFLECTED SIGNALS

Results

The amplitude reflection coefficients were computed for each of the three run leg sections shown in Fig. 10. The amplitude variability of the successive reflected signals was, in general, quite large. Each successive signal represented a nominal shift in the associated reflection area of about 4.9 feet. The pulse length was 1.3 msec so that the area associated with each reflected pulse was to a large extent independent of the preceding pulses. The reflected pulse envelopes were similar in character to those of the direct pulses. Follow-on reverberation was very small and was generally indistinguishable from the interference noise background discussed previously. A plot of these coefficients versus grazing angle suggested the existence of some periodicity. This relationship was confirmed when the raw computation results were smoothed by means of a 5-point moving average technique. The smoothed results are plotted in Figs. 11, 14 and 17 as a function of the grazing angle and in Figs. 12, 15 and 18 as a function of the position (shift) of the reflection area. The ordinate, in dB, represents 20 times the log to the base 10 of the numerical average of successive amplitude reflection coefficients, plotted at the abscissa corresponding to the central raw data value. The corresponding standard deviation of the reflected pulse amplitude is also plotted in Figs. 11, 14 and 17 as a function of the pulse interval. Each pulse interval has a time value of 2 sec, during which period the reflection area is shifted by about 5 ft.

The measure of variability is provided by the standard deviation of the differences $X_n - X_{n-j}$, where n corresponds to the sequential order number of the data and j is the sequence interval, 1 to 5 in this case. These differences are based on amplitude data corrected for the variation in absolute level due to range change effects and on the results of the computation converted to decibels.

Because of the geometry of the experimental runs, no ice profile measurements were made in exactly the positions corresponding to the reflection areas for the respective runs. However, profiles which are believed to be representative of those which existed in the respective reflection areas are presented in Figs. 13, 16 and 19, which correspond to data sets 6, 7 and 9. The corresponding slope statistics are shown, again as a function of interval distance, over the ensemble of profile data for each profile. The slope of the multi-year "flat" ice has a mean of essentially zero, taken over all interval distances, and has a typical standard deviation of about 3° at the 5-ft sample interval corresponding to the reflection area shift distance. At the 8-ft distance

corresponding to the acoustic pulse length, the standard deviation is about 2-1/2°. A similar profile (Fig. 20), corresponding to the section of the run trajectory labeled ROUGH ICE PROFILE in Fig. 10, indicates a slope standard deviation of 27° and 22-1/2° at the sampling intervals referred to above. Simple assumptions of nominal specular reflection from a horizontal surface would not, of course, apply to measurements made in this area.

Discussion

The mean value of the grand ensemble of reflection coefficient data presented here is very close to 0 dB, or unity. This is the expected value for specular reflection from a flat mirror surface. The amplitude reflection coefficient plots indicate a marked periodicity when plotted not only as a function of grazing angle but also as a function of distance, or movement, of the zone of reflection. This coefficient varies typically about ±6 dB from its mean value, as shown in the plots. The period of this variation shows more consistency when viewed as a function of the reflection zone shift than as a function of the nominal grazing angle. (See Figs. 11 and 12, in which reflectivity data obtained at grazing angles near 10° appear scattered in Fig. 11 when plotted versus grazing angle but become well ordered in Fig. 12 when plotted as a function of distance.) A review of Figs. 12, 15 and 18 indicates this periodic variation has a typical wavelength of 50 to 100 feet. The logical assumption is that the periodicity is related to the waviness of the water-ice interface.

While a rough estimate of the characteristic wavelength of the reflection coefficient variation can be discerned from the profiles of Figs. 12, 15 and 18, a similar judgment based on the profiles of Figs. 13, 16 and 19 is more difficult to make. A spectrum analysis was made of both the amplitude reflection coefficient data and the water-ice interface profile data of the latter set of figures. In agreement with the rough estimate, primary peaks were noted in the reflection coefficient power spectra at a frequency corresponding to a wavelength of 80 ft in data sets 7 and 9 and 70 ft in data set 6, which represents a smaller sample. The profile data spectrum analysis revealed the presence of three predominant, long wavelength peaks in the power spectra, and then a succeeding group of low level peaks corresponding to wavelengths from 51 to 107 ft with an integrated average peaking at a wavelength of 77.5 ft. This result suggests a relationship between the reflection coefficient and the water-ice profile that is more than fortuitous.

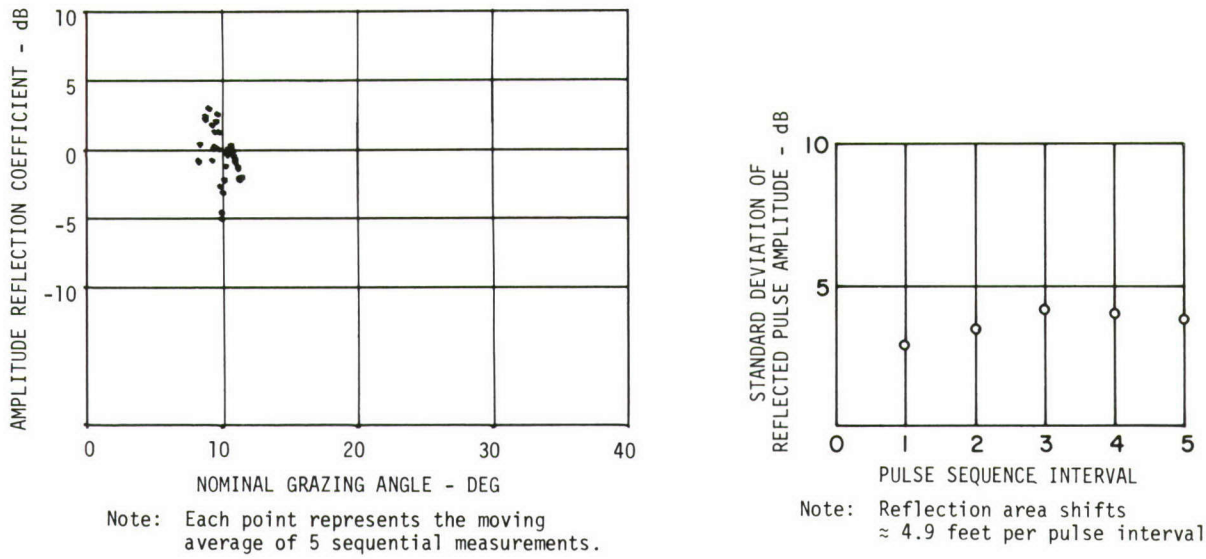

Figure 11. Mean Amplitude Reflection Coefficient as a Function of Grazing Angle, Fluctuation Properties, Data Set No. 6.

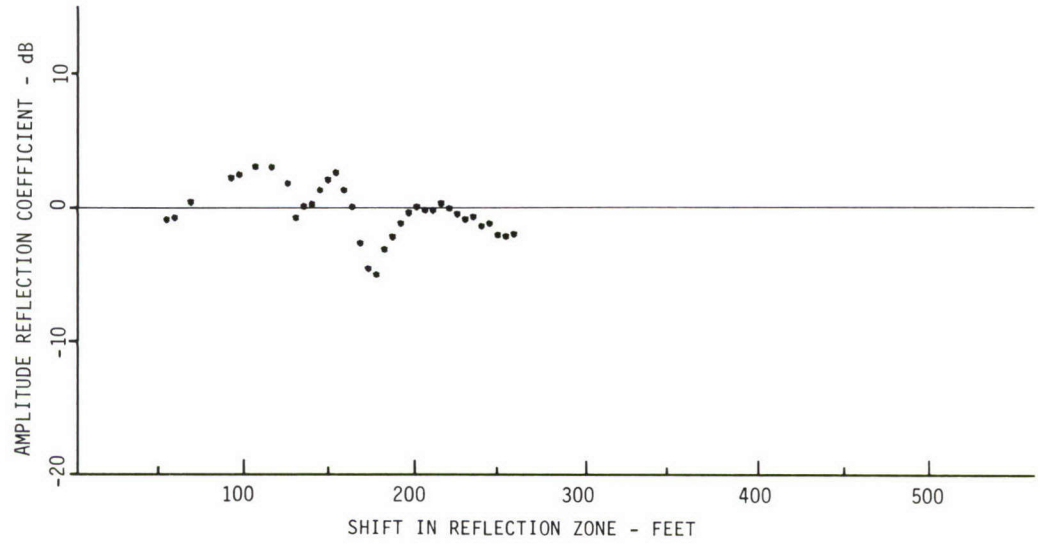

Figure 12. Mean Amplitude Reflection Coefficient as a Function of Reflection Zone Shift Distance, Data Set No. 6.

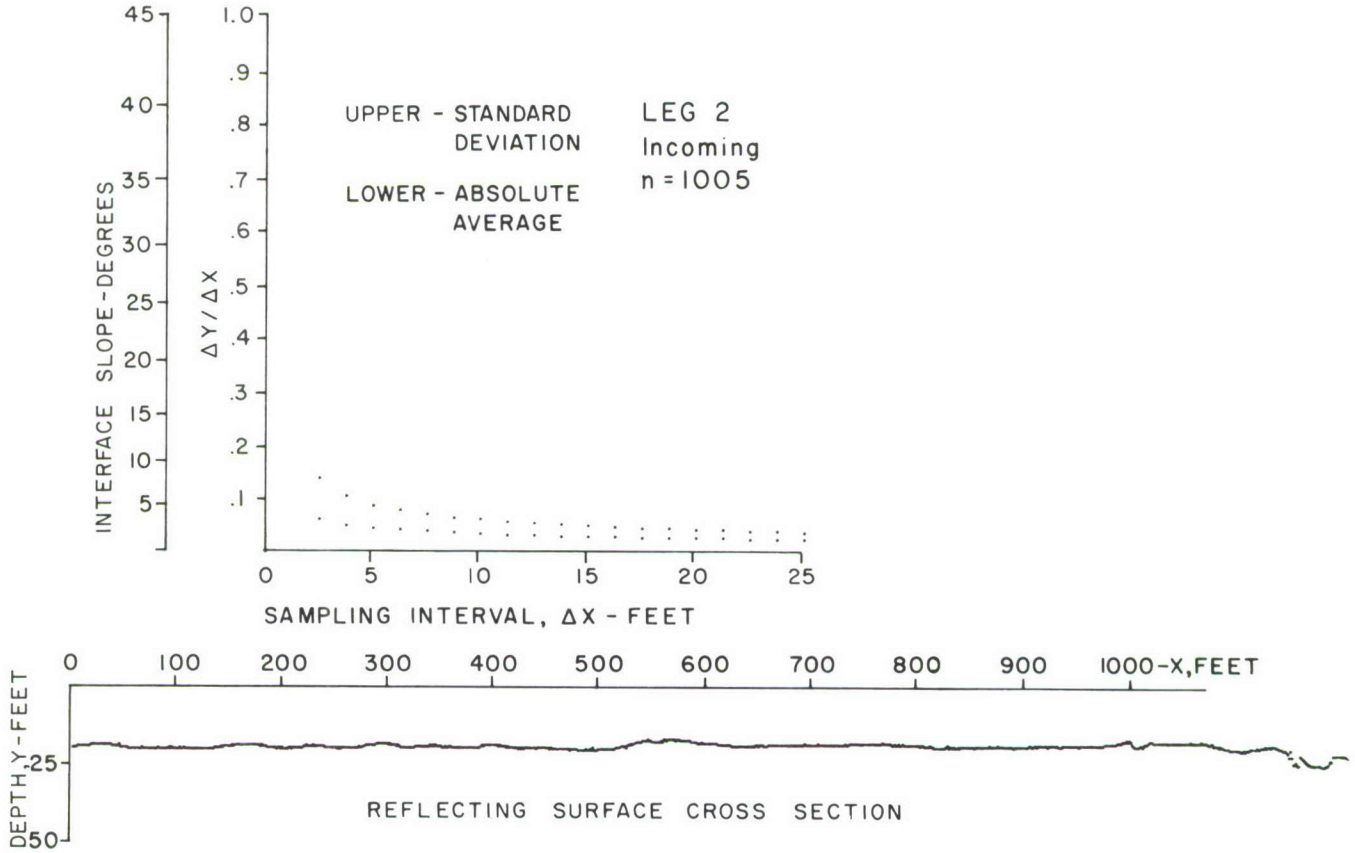

Figure 13. Typical Water-Ice Interface Cross Section and Slope Properties, Data Set No. 6.

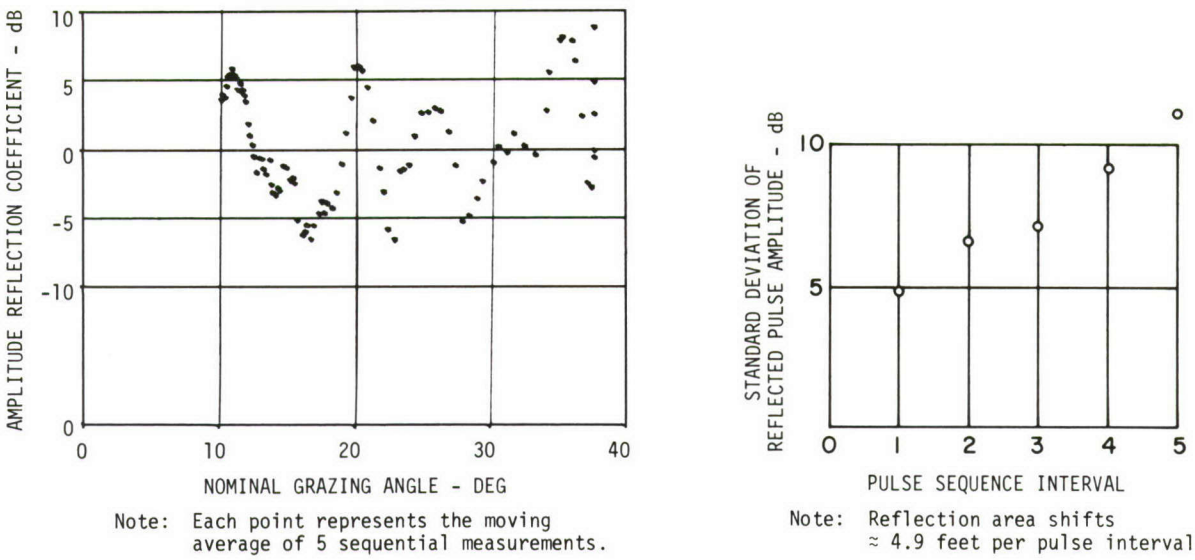

Figure 14. Mean Amplitude Reflection Coefficient as a Function of Grazing Angle, Fluctuation Properties, Data Set No. 7.

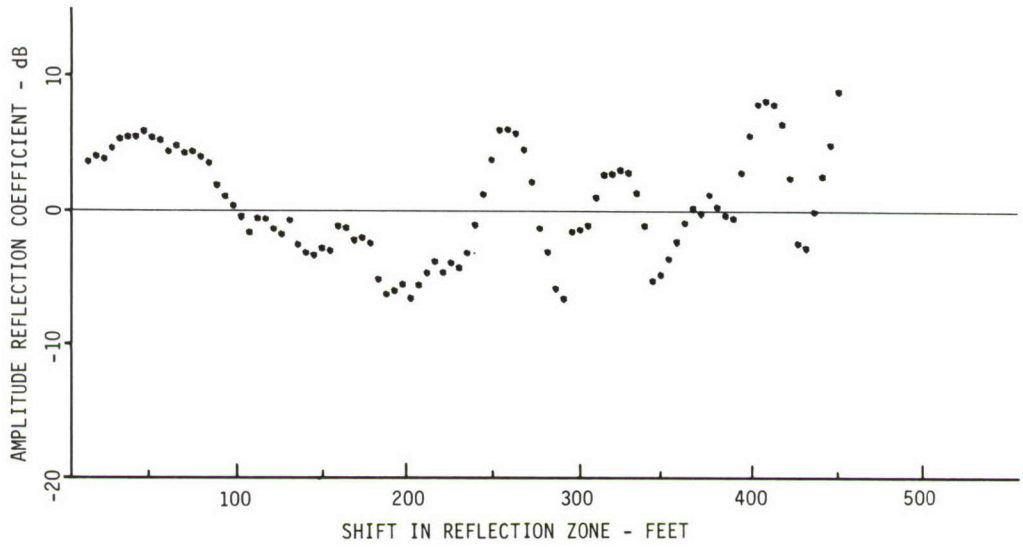

Figure 15. Mean Amplitude Reflection Coefficient as a Function of Reflection Zone Shift Distance, Data Set No. 7.

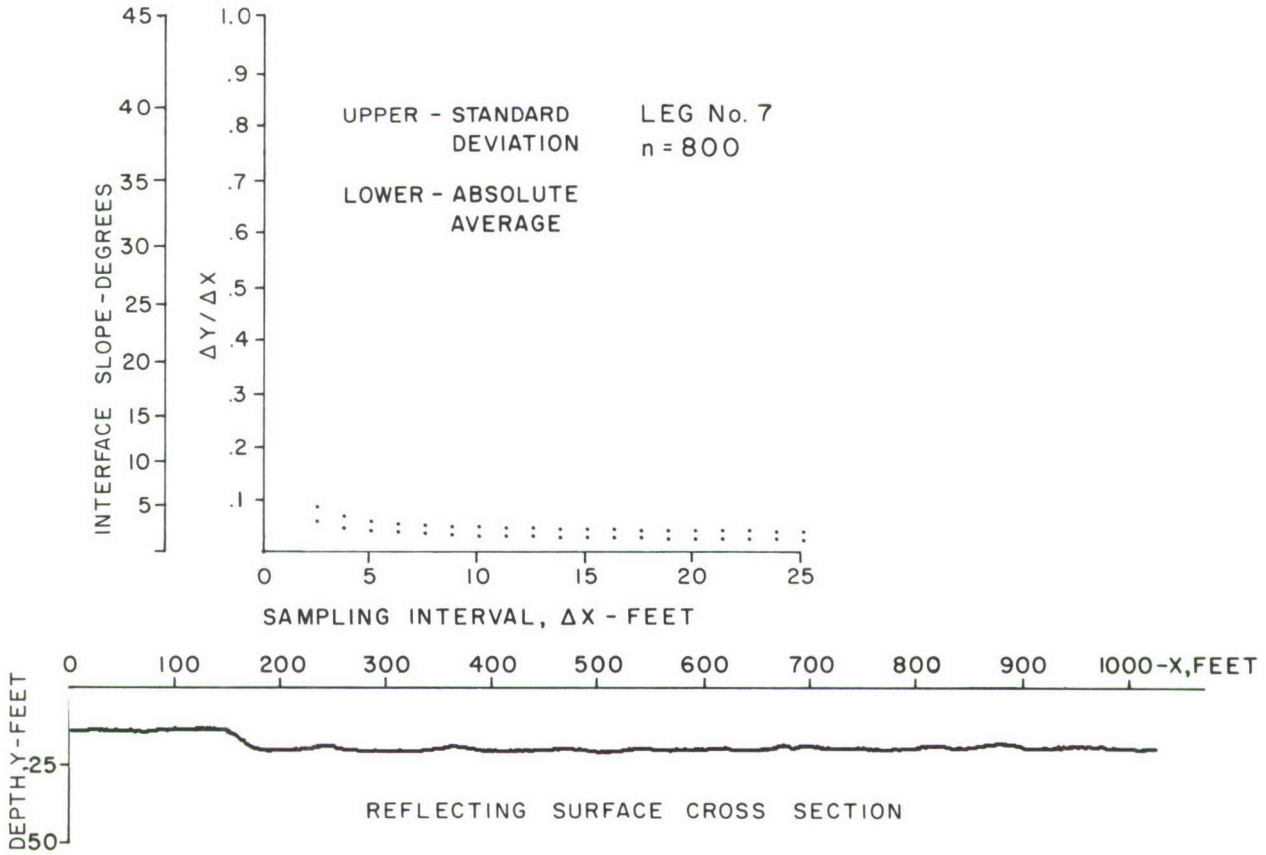

Figure 16. Typical Water-Ice Interface Cross Section and Slope Properties, Data Set No. 7.

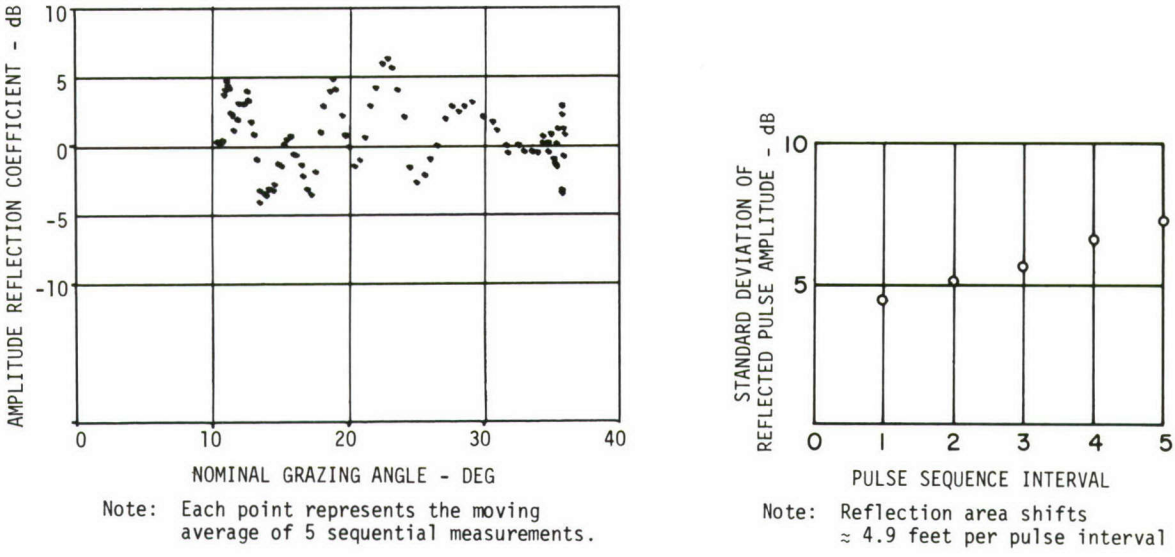

Figure 17. Mean Amplitude Reflection Coefficient as a Function of Grazing Angle, Fluctuation Properties, Data Set No. 9.

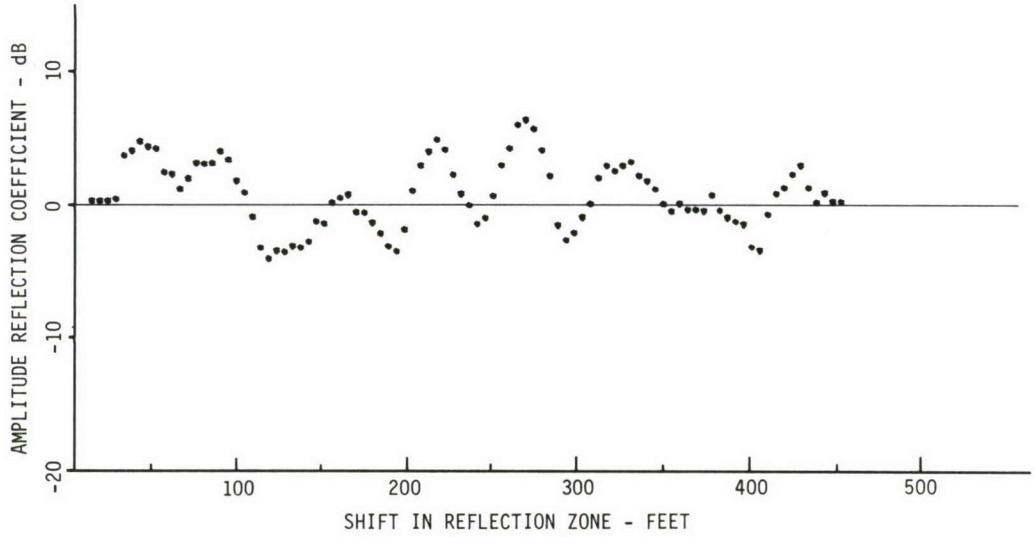

Figure 18. Mean Amplitude Reflection Coefficient as a Function of Reflection Zone Shift Distance, Data Set No. 9.

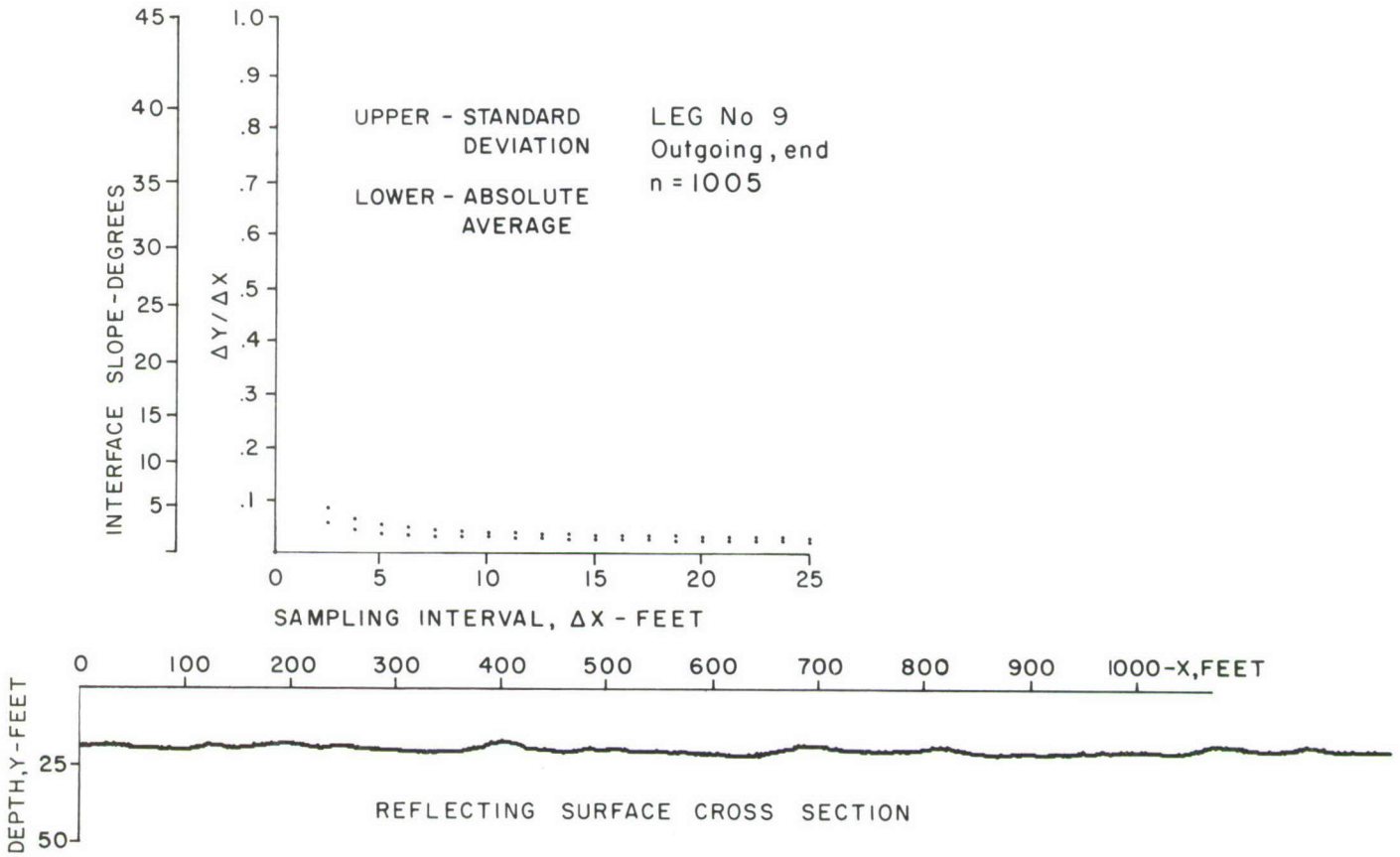

Figure 19. Typical Water-Ice Interface Cross Section and Slope Properties, Data Set No. 9.

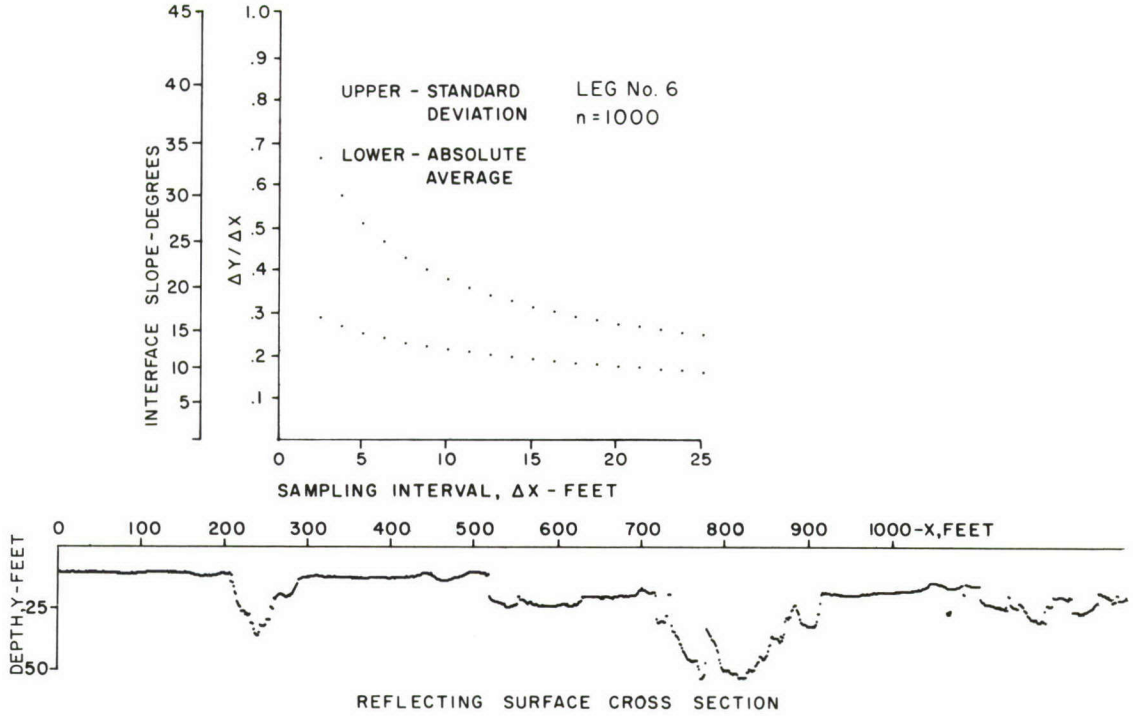

Figure 20. Example of Typical Water-Ice Interface Cross Section and Slope Properties for Rough Ice (Ridged).

A question now arises regarding the mechanism responsible for an amplitude reflection coefficient greater than unity--a measured value less than unity can always be explained in terms of a loss process. Here, a logical answer is that the undulating shape of the reflecting interface must be such that signal enhancement due to focusing is present. The question to be answered is whether the dimensional properties of the water-ice interface support such a hypothesis.

Referring to Fig. 21, in which there is a transmitter at F' and a receiver at F, the condition for focusing demands that the path length F'-P-F be constant and that the locus of P describe the surface of interest. The radius of curvature, R, at a selected point, P, describes the required surface contour for focusing to occur. The locus is an ellipise described by the equation

$$\frac{x^2}{a^2} + \frac{y^2}{b^2} = 1 \quad , \qquad (6)$$

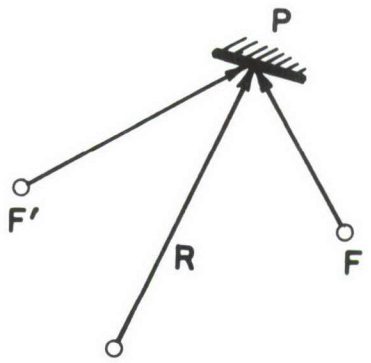

Figure 21. Locus of P with Radius of Curvature R Must Satisfy Condition that Distance F'-P-F Equals a Constant.

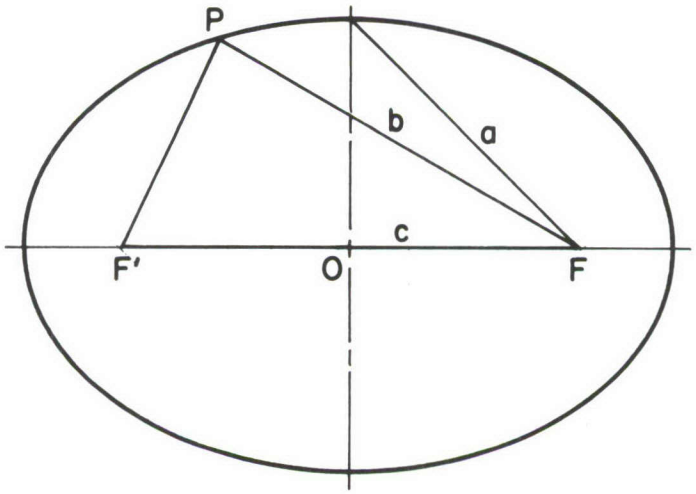

Figure 22. Locus of Points Satisfying Focusing Criteria, an Ellipse.

which follows the notation of Fig. 22. The radius of curvature of the locus at a selected point is

$$R = \frac{\left[1+\left(\frac{dy}{dx}\right)^2\right]^{3/2}}{\frac{d^2y}{dx^2}} \quad . \tag{7}$$

Solving Eq. (6) for y, we have

$$y = b\left(1 - \frac{x^2}{a^2}\right)^{\frac{1}{2}} \quad . \tag{8}$$

Taking the first and second derivatives,

$$\frac{dy}{dx} = -\frac{bx}{a^2}\left(1 - \frac{x^2}{a^2}\right)^{-\frac{1}{2}} \tag{9}$$

and

$$\frac{d^2y}{dx^2} = -\frac{b}{a^2}\left[\left(1 - \frac{x^2}{a^2}\right)^{-\frac{1}{2}} + \frac{x^2}{a^2}\left(1 - \frac{x^2}{a^2}\right)^{-3/2}\right] . \tag{10}$$

The separation distance between the transmitter and the receiver for the data presented in this report varied between 100 and 500 yd, and the average depth of the transmitter and the receiver below the reflecting surface was 110 ft. It is convenient to evaluate the radius of curvature for these two geometries at x = 0, a point midway between the two acoustic elements. From Fig. 22, 2c is equal to the horizontal separation range between the acoustic elements, which we will call R_H.

By inspection of Fig. 22, and substituting,

$$a^2 = b^2 + c^2 = b^2 + \frac{R_H^2}{4} \quad . \tag{11}$$

In the special case of x = 0, Eq. (7) reduces to

$$R = -\frac{a^2}{b} \tag{12}$$

so that at b = 110 feet and R_H = 300 feet

$$R = -314 \text{ feet},$$

and at b = 110 feet and R_H = 1500 feet

$$R = -5223 \text{ feet}.$$

The negative sign indicates a concave curvature, viewed from the x-axis below the locus.

The computed curvatures which satisfy perfect focusing are quite large and can easily be met by the interface conditions over the small area associated with the pulse length employed. The focusing gains implicit in the measured reflection coefficients are relatively modest compared to the gains potentially available under ideal focusing conditions.

The amplitude of the ice waviness that would be associated with focusing conditions can now be examined. Assuming a sinusoidal surface of wavelength λ, the amplitude is defined by

$$y = A \sin 2\pi \frac{x}{\lambda} \quad . \tag{13}$$

Then

$$\frac{dy}{dx} = A \frac{2\pi}{\lambda} \cos 2\pi \frac{x}{\lambda} \tag{14}$$

and

$$\frac{d^2y}{dx^2} = - A \left(\frac{2\pi}{\lambda}\right)^2 \sin 2\pi \frac{x}{\lambda} \quad . \tag{15}$$

The radius of curvature of this surface at $dy/dx = 0$, or $x = 1/4\ \lambda$, is found by substituting in Eq. (7) to give

$$R = - \frac{1}{A \left(\frac{2\pi}{\lambda}\right)^2} \quad . \tag{16}$$

We have defined the radius of curvature for focused reflection at this same slope in Eq. (12). Equating Eqs. (12) and (16) and solving for A, the amplitude of the sine wave, we find

$$A = \frac{b}{a^2 \left(\frac{2\pi}{\lambda}\right)^2} \quad , \tag{17}$$

where

$$a^2 = b^2 + (R_H^2/4)$$

b = average transducer depth

R_H = transducer separation in x.

The solution to this equation for b = 110 feet, and a value for λ of 80 ft based on the spectrum analyses of the amplitude reflection coefficient data and the profile spectra, is shown in Fig. 23. The ordinate is the single amplitude, A, defined by Eq. (13). The required amplitude necessary to satisfy the curvature requirements associated with perfect focusing once in each cycle for a continuous sinusoidal surface under the experimental conditions is shown to be small, on the order of 0.1 ft at the average measurement distance. This small amplitude explains why the power spectra peaks of the profile analyses which were correlated to the reflectivity spectra peaks were of such low value. It is apparent that the ice elevation resolution necessary to define the ice profile and reflectivity interaction were close to the quantization limits employed in this experiment.

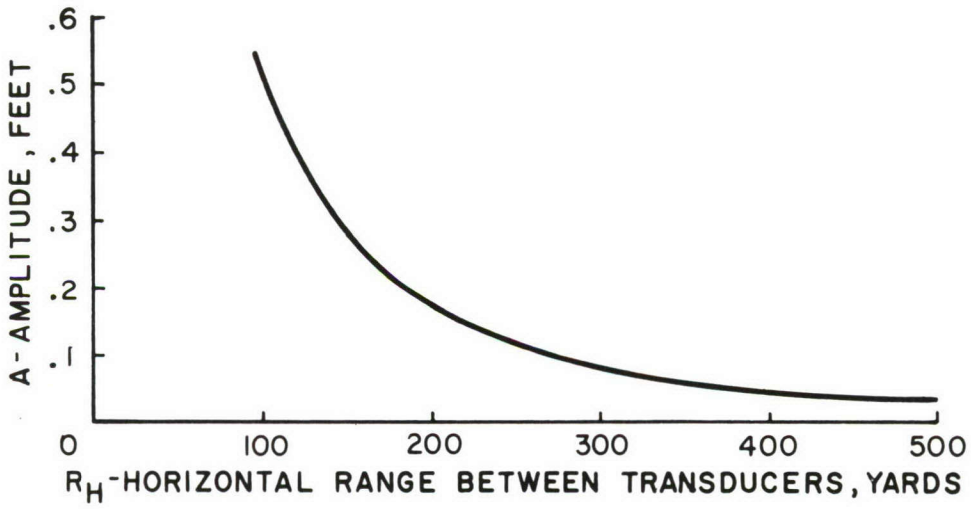

Figure 23. Amplitude of Sinusoidal Surface Which Satisfies Focusing Conditions.

For the above reasons, we believe that ordered variation in ice-reflected signals at shallow grazing angles can be expected, and that the amplitude of this variation will be dependent upon the nature of the ice undersurface. The ordered variation referred to here is the average reflected signal variation with reflection zone changes. The data also showed typical reflected signal pulse-to-pulse variations about these averaged values of a nominally 5 dB standard deviation. A knowledge of this dependency is important when designing validation logic for arctic

communication or tracking systems in which geometry permits the reflected pulses to overlap the direct path transmission. These results apply specifically to frequencies near 50 kHz but are an indication of what may be expected at similar acoustic-wavelength-to-surface-roughness ratios.

ATTENUATION COEFFICIENT

Measurement

The direct path attenuation coefficient at 50 kHz was determined from measurement of the direct path signal level at varying ranges. The geometry of Fig. 9 describing direct path propagation applies. The signal level, SL, at the receiving hydrophone is

$$SL = S - \delta_t - H - \delta_r \qquad (18)$$

where

S = the on-axis source level of the projector

δ_t = the number of dB down (on projector beam pattern) for off-axis transmission

δ_r = the number of dB down (on receiving hydrophone beam pattern) for off-axis reception

H = the spreading loss plus the attenuation loss due to the presence of the water medium.

The term H includes both the geometrical losses due to divergence of the signal with distance from the source and the attenuation loss due to the presence of a medium. The latter term is generally expressed as a coefficient giving loss in dB per kiloyard. The attenuation coefficient and the absorption coefficient are often used synonymously, but, strictly speaking, the attenuation coefficient includes the absorption coefficient and all other nongeometric losses as well. At moderate ranges, the spreading (or geometric loss) is generally assumed to be spherical, thus obeying a 20 log R falloff with range when expressed in decibel form.

In this experiment, the vertical velocity profile was obtained from daily CTD drops as previously discussed. First, the measured conductivity of the sea water was converted to salinity using the measured temperature. The mean temperature along the transmission path was -1.62°C and the computed salinity 31.9‰. The average pressure along the path was 4.8 atmospheres. Then the sound velocity profile was computed based on the individual

CTD data measurements made at depth intervals of about 1/2 ft, using Wilson's equation (Ref. 7). The sound velocity profile was used in computing the refraction loss as previously described. The departure from isovelocity conditions was slight and the refraction corrections were within 0.1 dB of the 20 log R value. The ray angles at both the projector and the receiver hydrophones were computed, considering the refraction effect, and the corresponding transducer directivity correction was made.

Letting $20 \log R_n + C_n$ represent the corrected spreading loss term applicable to each measurement and αR_n the attenuation loss at range R_n, substituting in Eq. (18) and re-arranging terms gives

$$\alpha R_n = -[20 \log R_n + C_n + \delta_{tn} + \delta_{rn} + SL] + S \ . \qquad (19)$$

For SL, we may substitute $20 \log V_D + B$, where V_D is the voltage induced in the receiving transducer and B is its receiving sensitivity in dBV//μbar.

The attenuation coefficient, α, is found by plotting the attenuation parameter αR_n versus R_n and least square fitting a line. The slope of that line yields α, independently of "unknown" values of S and B.

Results

The least square fit to 94 measurements made over a range that varied from 96.5 yd to 414.3 yd gave an α of 11.0 dB per kiloyard, with a standard error of 0.72 dB with respect to the least square regression line and a correlation coefficient of 0.83. The data set was truncated by 10, 20, and 30 points at either end of the distribution to test the sensitivity of the slope, hence α, to the data distribution. The greatest change in α occurred when 30 points were removed at the maximum range. This change resulted in an α of 10.03 dB per kiloyard, an increase in the standard error to 0.81 dB and a decrease in the correlation coefficient to 0.60. The zero range intercept remained constant within 0.17 dB in all cases. The best estimate of α is thus considered to be 11.0 dB per kiloyard for the indicated measurement conditions at the frequency of 50 kHz.

Discussion

The attenuation coefficient measured in this experiment is compared with the results of other investigators--Schulkin and Marsh (Ref. 4), Murphy, Garrison and Potter (Ref. 8), and Greene in Ref. 5--in Fig. 24.

The early study by Murphy, Garrison and Potter (the APL-UW curve in the figure) utilized measurements at four frequencies--60, 142, 272 and 467 kHz--over a range of temperature and salinity conditions. Schulkin and Marsh also combined theory with a large number of propagation measurements made in programs of the U.S. Navy Underwater Sound Laboratory.

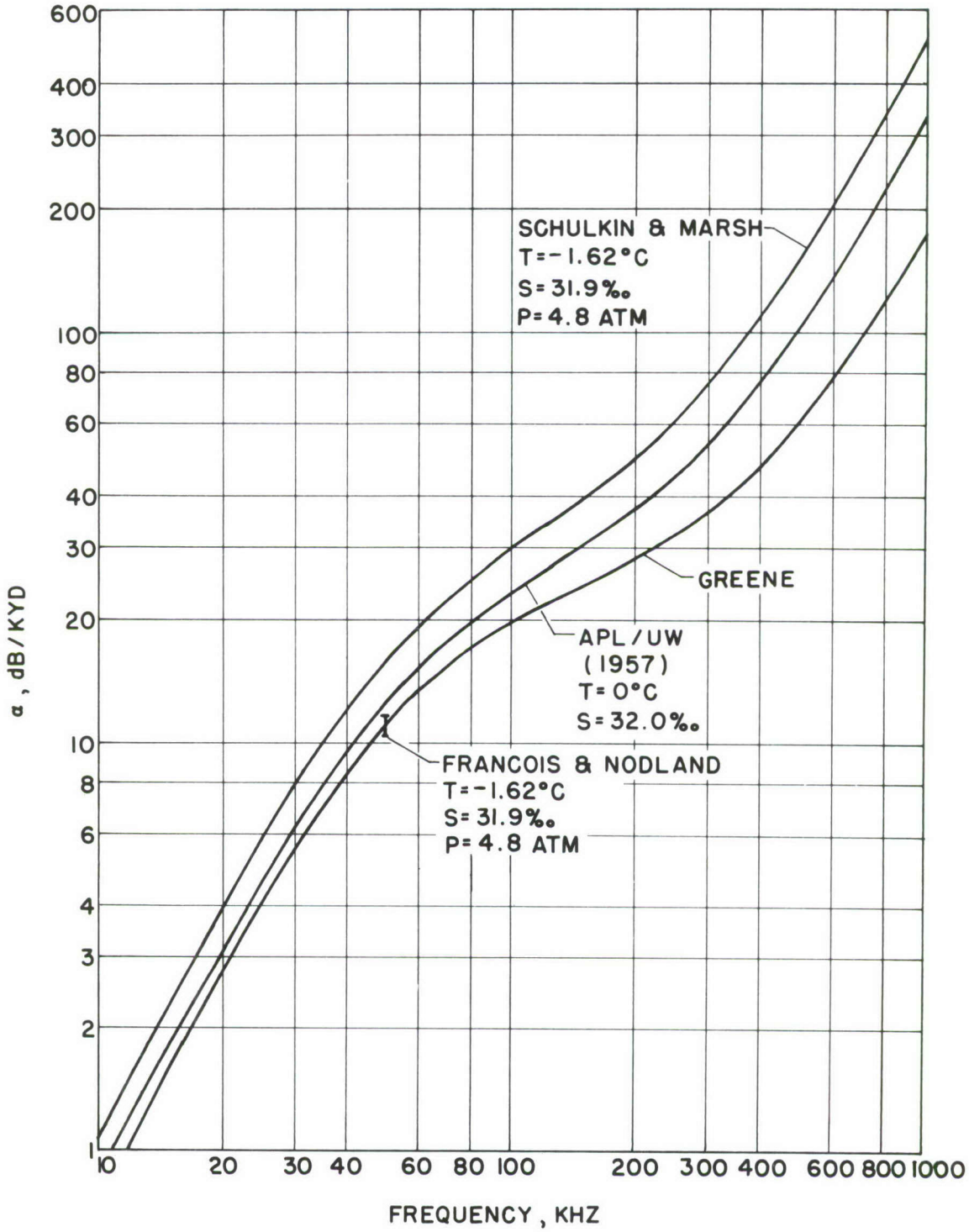

Figure 24. Sea Water Attenuation for Arctic Medium Conditions.

These measurements covered frequencies from 2 to 24 kHz over ranges as great as 24,000 yards in the North Atlantic at various times of the year. Data from other investigations were used to provide a fit at the middle frequencies. Neither of the above studies is known to include data at <0°C temperatures. This is important, because one of the areas of greatest uncertainty in the application of the theory is the relaxation frequency dependence upon temperature (and salinity). As can be seen from Fig. 24, the transition zone from the region in which relaxation processes dominate the attenuation coefficient (low frequencies) to the region in which viscosity effects predominate (high frequencies) is in the mid-frequency region utilized for naviation, tracking range operations, and high resolution, small size sonar applications.

Greene's curve is for generalized environmental conditions under mid-arctic, ice-covered seas. His data were taken over a wide range of frequencies encompassing the transition region. The measurement made in this experiment, perhaps fortuitously, is in almost exact agreement with his predicted value for typical, near-ice propagation path conditions. The measured attenuation coefficient at 50 kHz under the indicated environmental conditions is some 5 dB per kiloyard less than that predicted by the Schulkin and Marsh equation and 1.6 dB per kiloyard less than the previous APL-UW predictions. These discrepancies are not trivial when one considers the resulting effect on the performance of a sonar system designed for operation at a range of 1000 yards or greater.

SUMMARY

The amplitude of acoustic pulses reflected from the undersurface of unridged multi-year sea ice at small grazing angles was found to have an overall average value equal to that of the direct path signal. Average reflected signals varied by typically ±6 dB, however, as the source was moved horizontally with respect to the receiver, thus shifting the reflection zone. The period of this fluctuation was related to a 50-100 ft wavelength component in the water-ice interface roughness spectra. Short term fluctuations with a standard deviation on the order of 5 dB were superimposed on the periodic averaged signal level.

When signal reflection occurred in ridged ice areas, only very short sequences of the reflected signal were received, since the reflected signals either were cut off by the geometry of the pressure ridge keels or were scattered by the jumble of fractured ice at the bottom and sloped sides of the keels. The behavior of signals reflected from the "flat" ice areas between ridges, while not analyzed in this report, was observed to have the same general characteristics as those reported herein.

The direct path attenuation coefficient determined from this experiment was 11.0 dB per kiloyard at 50 kHz. The standard error of this measurement was 0.72 dB, which indicates that over ranges to 500 yards the direct path signal fluctuations ascribable to the medium were small.

REFERENCES

1. R.E. Francois and W.E. Nodland, "Unmanned Arctic Research Submersible (UARS) System Development and Test Report," APL-UW 7219, Applied Physics Laboratory, University of Washington, 11 September 1972.

2. R. E. Francois, "The Unmanned Arctic Research Submersible System," Marine Technology Society Journal, Vol. 7, No. 1, January-February 1973.

3. M.P. Langleben and E.R. Pounder, "Reflection of Sound at the Water-Ice Interface," Part II of Report S-16, Macdonald Physics Laboratory, McGill University, May 1970.

4. M. Schulkin and H. W. Marsh, "Sound Absorption in Sea Water," The Journal of the Acoustical Society of America, Vol. 34, No. 6, p. 864, June 1962.

5. Greene, as quoted by B.P. Miller in "A Study of Submarine-Launched ASW Weapons in the Arctic (U)," TR 69-65, AC Electronics-Defense Research Laboratories, December 1969 (Confidential).

6. P. Marsh and A.B. Poynter, "Digital Computer Programs for Analyzing Acoustic Search Performance in Refractive Waters, NUC Programs 800000 and 800001," NUC TP 164, 2 vols., Naval Undersea Research and Development Center, December 1969.

7. W.D. Wilson, "Extrapolation of the Equation for the Speed of Sound in Sea Water," The Journal of the Acoustical Society of America, Vol. 34, No. 6, p. 866, June 1962.

8. S.R. Murphy, G.R. Garrison and D.S. Potter, Further results of work reported in "Sound Absorption at 50 to 500 kc from Transmission Measurements in the Sea," The Journal of the Acoustical Society of America, Vol. 30, No. 9, p. 871, September 1958.

UNCLASSIFIED

Security Classification

DOCUMENT CONTROL DATA - R&D

(Security classification of title, body of abstract and indexing annotation must be entered when the overall report is classified)

1. ORIGINATING ACTIVITY *(Corporate author)*

Applied Physics Laboratory, University of Washington, 1013 NE 40th, Seattle, Wash. 98105

2a. REPORT SECURITY CLASSIFICATION

Unclassified

2b. GROUP

3. REPORT TITLE

ARCTIC ACOUSTIC MEASUREMENTS AT 50 kHz

4. DESCRIPTIVE NOTES *(Type of report and inclusive dates)*

5. AUTHOR(S) *(Last name, first name, initial)*

Francois, Robert E.
Nodland, Wayne E.

6. REPORT DATE	7a. TOTAL NO. OF PAGES	7b. NO. OF REFS
31 August 1973	35	8

8a. CONTRACT OR GRANT NO.	9a. ORIGINATOR'S REPORT NUMBER(S)
N00017-71-C-1305	APL-UW 7313
b. PROJECT NO.	
c.	9b. OTHER REPORT NO(S) *(Any other numbers that may be assigned this report)*
d.	

10. AVAILABILITY/LIMITATION NOTICES

Approved for public release; distribution unlimited.

11. SUPPLEMENTARY NOTES	12. SPONSORING MILITARY ACTIVITY
	Naval Ordnance Laboratory White Oak Silver Spring, Maryland 20910

13. ABSTRACT

An acoustic transmission experiment was conducted in conjunction with development operations of the Unmanned Arctic Research Submersible (UARS) system off Fletcher's Ice Island (T-3). Transmissions from a low directivity, 50-kHz projector on the submersible (part of the UARS acoustic tracking system) were received at transducers suspended beneath the ice and then recorded. The profile of the ice immediately above the UARS was measured throughout the run and the UARS acoustic tracking system provided complete knowledge of the changing measurement geometry. The data were analyzed to yield the amplitude reflection coefficient as a function of the nominal grazing angle with the ice undersurface and the shift in reflection area, the sea water attenuation coefficient, and signal fluctuation statistics. The amplitude reflection coefficient was found to be highly variable and independent of grazing angle for angles from 10° to 40°; the reflected signal had short-term fluctuations with a standard deviation on the order of 5 dB. The mean coefficient, however, varied about unity by typically ±6 dB in a somewhat periodic manner which was related to a secondary 50 to 100 foot wavelength component present in the measured ice roughness spectra. The measured attenuation coefficient at a frequency of 50 kHz, a temperature of -1.62°C, a salinity of 31.9‰, and a pressure of 4.8 atmospheres was 11.0 dB per kiloyard. This value confirms Greene's arctic measurements but is some 5 dB less than that predicted by Schulkin and Marsh. The standard error of this measurement was 0.72 dB, which indicates that over the ranges used in the experiment (500-yd maximum) the direct path signal fluctuations ascribable to the medium were small.

DD FORM 1 JAN 64 1473

UNCLASSIFIED

Security Classification

14. KEY WORDS	LINK A		LINK B		LINK C	
	ROLE	WT	ROLE	WT	ROLE	WT
Reflectivity of Sea Ice Attenuation Fluctuation of ice-reflected acoustic energy						

INSTRUCTIONS

1. ORIGINATING ACTIVITY: Enter the name and address of the contractor, subcontractor, grantee, Department of Defense activity or other organization *(corporate author)* issuing the report.

2*a*. REPORT SECURITY CLASSIFICATION: Enter the overall security classification of the report. Indicate whether "Restricted Data" is included. Marking is to be in accordance with appropriate security regulations.

2*b*. GROUP: Automatic downgrading is specified in DoD Directive 5200.10 and Armed Forces Industrial Manual. Enter the group number. Also, when applicable, show that optional markings have been used for Group 3 and Group 4 as authorized.

3. REPORT TITLE: Enter the complete report title in all capital letters. Titles in all cases should be unclassified. If a meaningful title cannot be selected without classification, show title classification in all capitals in parenthesis immediately following the title.

4. DESCRIPTIVE NOTES: If appropriate, enter the type of report, e.g., interim, progress, summary, annual, or final. Give the inclusive dates when a specific reporting period is covered.

5. AUTHOR(S): Enter the name(s) of author(s) as shown on or in the report. Enter last name, first name, middle initial. If military, show rank and branch of service. The name of the principal author is an absolute minimum requirement.

6. REPORT DATE: Enter the date of the report as day, month, year; or month, year. If more than one date appears on the report, use date of publication.

7*a*. TOTAL NUMBER OF PAGES: The total page count should follow normal pagination procedures, i.e., enter the number of pages containing information.

7*b*. NUMBER OF REFERENCES: Enter the total number of references cited in the report.

8*a*. CONTRACT OR GRANT NUMBER: If appropriate, enter the applicable number of the contract or grant under which the report was written.

8*b*, 8*c*, & 8*d*. PROJECT NUMBER: Enter the appropriate military department identification, such as project number, subproject number, system numbers, task number, etc.

9*a*. ORIGINATOR'S REPORT NUMBER(S): Enter the official report number by which the document will be identified and controlled by the originating activity. This number must be unique to this report.

9*b*. OTHER REPORT NUMBER(S): If the report has been assigned any other report numbers *(either by the originator or by the sponsor)*, also enter this number(s).

10. AVAILABILITY/LIMITATION NOTICES: Enter any limitations on further dissemination of the report, other than those imposed by security classification, using standard statements such as:

(1) "Qualified requesters may obtain copies of this report from DDC."

(2) "Foreign announcement and dissemination of this report by DDC is not authorized."

(3) "U. S. Government agencies may obtain copies of this report directly from DDC. Other qualified DDC users shall request through

_____."

(4) "U. S. military agencies may obtain copies of this report directly from DDC. Other qualified users shall request through

_____."

(5) "All distribution of this report is controlled. Qualified DDC users shall request through

_____."

If the report has been furnished to the Office of Technical Services, Department of Commerce, for sale to the public, indicate this fact and enter the price, if known.

11. SUPPLEMENTARY NOTES: Use for additional explanatory notes.

12. SPONSORING MILITARY ACTIVITY: Enter the name of the departmental project office or laboratory sponsoring *(paying for)* the research and development. Include address.

13. ABSTRACT: Enter an abstract giving a brief and factual summary of the document indicative of the report, even though it may also appear elsewhere in the body of the technical report. If additional space is required, a continuation sheet shall be attached.

It is highly desirable that the abstract of classified reports be unclassified. Each paragraph of the abstract shall end with an indication of the military security classification of the information in the paragraph, represented as *(TS), (S), (C), or (U)*.

There is no limitation on the length of the abstract. However, the suggested length is from 150 to 225 words.

14. KEY WORDS: Key words are technically meaningful terms or short phrases that characterize a report and may be used as index entries for cataloging the report. Key words must be selected so that no security classification is required. Identifiers, such as equipment model designation, trade name, military project code name, geographic location, may be used as key words but will be followed by an indication of technical context. The assignment of links, roles, and weights is optional.